Molecular Pharmacology Fast Forward. Published on April 30, 2009 as DOI: 10.1124/mol.109.056531
Molecular Pharmacology Fast Forward. Published on April 30, 2009 as doi:10.1124/mol.109.056531
This article has not been copyedited and formatted. The final version may differ from this version.

MOL # 56531

A Novel Selective Muscarinic Acetylcholine Receptor Subtype 1 (M_1 mAChR) Antagonist Reduces Seizures Without Impairing Hippocampal-Dependent Learning

Douglas J. Sheffler, Richard Williams, Thomas M. Bridges, Zixiu Xiang, Alexander S. Kane, Nellie E. Byun, Satyawan Jadhav, Mathew M. Mock, Fang Zheng, L. Michelle Lewis, Carrie K. Jones, Colleen M. Niswender, Charles D. Weaver, Craig W. Lindsley, and P. Jeffrey Conn

Departments of Pharmacology (D.J.S., R.W., T.M.B., Z.X., A.S.K., C.K.J., C.M.N., S.J., and P.J.C.), Chemistry (C.W.L.), Radiology and Radiological Sciences (N.E.B.), the Vanderbilt Program in Drug Discovery (R.W., S.J., C.K.J., C.M.N., C.D.W., C.W.L., and P.J.C.), and the Vanderbilt Institute of Chemical Biology (L.M.L., C.D.W., C.W.L., and P.J.C.), Vanderbilt University Medical Center, Nashville, TN 37232. Department of Pharmacology and Toxicology (M.M.M. and F.Z.), University of Arkansas Medical Center, Little Rock, AR 72205.

Downloaded from molpharm.aspetjournals.org at ASPET Journals on April 20, 2024

Copyright 2009 by the American Society for Pharmacology and Experimental Therapeutics.

Molecular Pharmacology Fast Forward. Published on April 30, 2009 as DOI: 10.1124/mol.109.056531
This article has not been copyedited and formatted. The final version may differ from this version.

MOL # 56531

Running Title: A Novel Selective M_1 mAChR Antagonist

****To whom correspondence should be addressed:**

P. Jeffrey Conn, Ph.D.

Dept. of Pharmacology, Light Hall (MRB-IV) Room 1215D, Vanderbilt University Medical Center, 2215 B Garland Avenue, Nashville, TN 37232

Tel.: 615-936-2478 Fax: 615-343-3088 E-mail: jeff.conn@vanderbilt.edu

Number of Text Pages: 47

Number of Tables: 1 (Plus 1 Supplemental)

Number of Figures: 11 (Plus 2 Supplemental)

Number of References: 40

Words in Abstract: 250

Words in Introduction: 674

Words in Discussion: 1295

Abbreviations: ACh, acetylcholine; CCh, carbachol; PD, Parkinson's Disease; CHO, Chinese Hamster Ovary; GPCR, G protein-coupled receptor; mAChRs, muscarinic acetylcholine receptors; M_1-M_5, muscarinic receptor subtypes; mGluR, metabotropic glutamate receptor; VU0255035, *N*-(3-oxo-3-(4-(pyridine-4-yl)piperazin-1-yl)propyl)benzo[c][1,2,5]thiadiazole-4 sulfonamide; NDMC, N-desmethylclozapine; [^{3}H]-NMS, l-[N-methyl-^{3}H]scopolamine; ERK, extracellular signal-regulated kinase; NMDA, N-methyl-D-aspartate; TBPB, 1-(1'-2-methylbenzyl)-1,4'-bipiperidin-4-yl)-1H-benzo[d]imidazol-2(3H)-one

Downloaded from molpharm.aspetjournals.org at ASPET Journals on April 20, 2024

Molecular Pharmacology Fast Forward. Published on April 30, 2009 as DOI: 10.1124/mol.109.056531
This article has not been copyedited and formatted. The final version may differ from this version.

Abstract

Previous studies suggest that selective antagonists of specific subtypes of muscarinic acetylcholine (ACh) receptors (mAChRs) may provide a novel approach for the treatment of certain CNS disorders, including epileptic disorders, Parkinson's disease, and dystonia. Unfortunately, previously reported antagonists are not highly selective for specific mAChR subtypes, making it difficult to definitively establish the functional roles and therapeutic potential for individual subtypes of this receptor subfamily. The M_1 mAChR is of particular interest as a potential target for treatment of CNS disorders. We now report the discovery of a novel selective antagonist of M_1 mAChRs, termed VU0255035. Equilibrium radioligand binding and functional studies demonstrate a greater than 75-fold selectivity of VU0255035 for M_1 mAChRs relative to M_2-M_5. Molecular pharmacology and mutagenesis studies indicate that VU0255035 is a competitive orthosteric antagonist of M_1 mAChRs, a surprising finding given the high level of M_1 mAChR selectivity relative to other orthosteric antagonists. Whole cell patch clamp recordings demonstrate that VU0255035 inhibits potentiation of NMDA receptor currents by the muscarinic agonist carbachol in hippocampal pyramidal cells. VU0255035 has excellent brain penetration *in vivo* and is efficacious in reducing pilocarpine-induced seizures in mice. Surprisingly, doses of VU0255035 that reduce pilocarpine-induced seizures do not induce deficits in contextual freezing, a measure of hippocampal-dependent learning that is disrupted by nonselective mAChR antagonists. Taken together, these data suggest that selective antagonists of M_1 mAChRs do not induce the severe cognitive deficits seen with non-selective mAChR antagonists and could provide a novel approach for the treatment certain of CNS disorders.

Downloaded from molpharm.aspetjournals.org at ASPET Journals on April 20, 2024

Molecular Pharmacology Fast Forward. Published on April 30, 2009 as DOI: 10.1124/mol.109.056531
This article has not been copyedited and formatted. The final version may differ from this version.

Introduction

Muscarinic acetylcholine receptors (mAChRs) are G protein-coupled receptors (GPCRs) that are widely expressed in the central nervous system (CNS) and are critical for the modulation of activity in multiple brain circuits (Langmead et al., 2008). Previous studies suggest that mAChRs play important roles in a broad range of CNS functions, including attention and cognitive function, nociception, regulation of sleep/wake cycles, motor control, and arousal. Furthermore, mAChR ligands have been proposed to have potential efficacy in a wide variety of CNS disorders, including chronic and neuropathic pain, sleep disorders, epilepsy, schizophrenia, Alzheimer's disease, Parkinson's disease (PD), and dystonia (Bymaster et al., 2003b; Langmead et al., 2008).

Based on the heterogeneous distribution and diverse physiological roles of mAChRs, the opportunity exists for developing therapeutic agents that selectively interact with individual mAChR subtypes involved in specific CNS functions. The mAChRs are members of the family A GPCRs and include five subtypes, termed M_1 - M_5. While each of the mAChR subtypes can couple to multiple signaling pathways in different systems, the M_1, M_3, and M_5 mAChR subtypes often couple to G_q and activate phopholipase C whereas M_2 and M_4 couple to $G_{i/o}$ and associated effector systems, such as ion channels and adenylyl cyclase (Felder et al., 2000; Langmead et al., 2008). Unfortunately, the orthosteric (ACh) binding site of the mAChR is highly conserved and this has led to difficulty in the development of highly selective ligands for individual mAChR subtypes (Felder et al., 2000). This lack of subtype-selective pharmacological reagents for mAChRs has prevented development of a clear understanding of the physiological roles of individual mAChR subtypes.

Downloaded from molpharm.aspetjournals.org at ASPET Journals on April 20, 2024

Molecular Pharmacology Fast Forward. Published on April 30, 2009 as DOI: 10.1124/mol.109.056531
This article has not been copyedited and formatted. The final version may differ from this version.

Of the mAChRs, M_1 is among the most heavily expressed in forebrain and midbrain regions and has been proposed to play important roles in memory and attention mechanisms, motor control, and regulation of sleep wake cycles (Felder et al., 2000). Based on the potential role of M_1 in seizure activity and motor control, it has been postulated that highly selective M_1 antagonists may have potential utility in the treatment of some epileptic disorders as well as certain movement disorders, including PD and dystonia (Hamilton et al., 1997; Pisani et al., 2007). Previous studies suggest that M_1 is not involved in most of the peripheral actions of mAChR ligands, suggesting that M_1-selective antagonists are not likely to induce the peripherally-mediated adverse effects of non-selective mAChR antagonists (Bymaster et al., 2003a; Langmead et al., 2008). However, mAChR antagonists have also been long known to induce severe impairments in cognitive function (Drachman and Leavitt, 1974). Based on the postulated roles of M_1 in different forms of learning and memory, it is possible that M_1-selective antagonists could induce impairments in cognitive function that are similar to those of non-selective mAChR antagonists. However, the role of M_1 mAChRs in the processes of memory acquisition and consolidation are not entirely clear. Interestingly, M_1 mAChR knockout mice display relatively subtle changes in cognitive function and hippocampal-dependent learning remains largely intact these animals (Anagnostaras et al., 2003; Miyakawa et al., 2001). Furthermore, studies with mice in which each of the other mAChR subtypes have been genetically deleted suggest that multiple mAChR subtypes participate in cholinergic regulation of learning and memory (see (Wess, 2004) for review). Based on these observations, it is possible that M_1-selective antagonists may provide a viable approach to treatment of certain CNS disorders and may not induce the adverse effects observed with non-selective mAChR antagonists. Unfortunately, the lack of highly selective antagonists of M_1 and other mAChR

Downloaded from molpharm.aspetjournals.org at ASPET Journals on April 20, 2024

Molecular Pharmacology Fast Forward. Published on April 30, 2009 as DOI: 10.1124/mol.109.056531
This article has not been copyedited and formatted. The final version may differ from this version.

subtypes has made it impossible to test this hypothesis. We now report discovery and detailed characterization of VU0255035 as a highly selective M_1 antagonist. The pharmacokinetic profile and CNS penetration of VU0255035 makes this compound well suited for *in vivo* studies in animal models. Interestingly, VU0255035 inhibits induction of generalized seizures by the mAChR agonist pilocarpine but does not mimic the cognitive-impairing effects of the mAChR antagonist scopolamine in a behavioral measure of hippocampal-dependent learning. Together, these data raise the exciting possibility that the use of selective M_1 mAChR antagonists as therapeutics may not induce severe cognitive deficits.

Downloaded from molpharm.aspetjournals.org at ASPET Journals on April 20, 2024

Molecular Pharmacology Fast Forward. Published on April 30, 2009 as DOI: 10.1124/mol.109.056531
This article has not been copyedited and formatted. The final version may differ from this version.

Materials and Methods

Cell culture and transfections. Chinese hamster ovary (CHO) cells stably expressing rat M_1 (rM_1) were purchased from the American Type Culture Collection (ATCC, Manassas, VA) and cultured following their recommendations. CHO cells stably expressing human M_2 (hM_2), hM_3, and hM_5 were generously provided by A. Levey (Emory Medical School, Atlanta, GA). rM4 cDNA, provided by T.I. Bonner (National Institutes of Health, Bethesda, MD), was used to stably transfect CHO-K1 cells purchased from the ATCC using Lipofectamine 2000 (Invitrogen, Carlsbad, CA). To make stable hM_2 and rM_4 cell lines for use in calcium mobilization assays, these cells were also stably transfected with a chimeric G protein (G_{qi5}) using Lipofectamine 2000. rM_1, hM_3, and hM_5 cells were grown in Ham's F-12 medium containing 10% heat-inactivated fetal bovine serum (FBS), 20 mM HEPES, and 50 µg ml–1 G418 sulfate. hM_2-G_{qi5} and rM_4-G_{qi5} cells were grown in the same medium also containing 500 µg/ml Hygromycin B. The rM1-Y381A CHO cell line was generated as previously described (Jones et al., 2008).

Primary High-Throughput Screening (HTS). The primary HTS was performed as previously described (Lewis et al., 2008).

Calcium Fluorescence Measurement. Chinese hamster ovary (CHO) cells expressing rM_1, hM_2-G_{qi5}, hM_3, rM_4-G_{qi5}, or hM_5 were plated at 40,000 cells per well in standard growth media (F12 (HAM), supplemented with 10% fetal bovine serum, and 20 mM HEPES) in 96 well plates twenty-four hours prior to assay and were incubated overnight at 37°C in 5% CO_2. On the day of the assay, media was removed and Calcium Assay Buffer (Hanks Balanced Salt Solution (HBSS;

Downloaded from molpharm.aspetjournals.org at ASPET Journals on April 20, 2024

Molecular Pharmacology Fast Forward. Published on April 30, 2009 as DOI: 10.1124/mol.109.056531
This article has not been copyedited and formatted. The final version may differ from this version.

Invitrogen, Carlsbad, CA), 20 mM HEPES, 2.5 mM Probenecid (Sigma, St. Louis, MO), pH 7.4) containing 1.8 µM Fluo4-AM dye (Invitrogen, Carlsbad, CA) was added. Cells were incubated for 45 min (37°C, 5% CO_2) for dye loading. Fluo4-AM dye was removed and replaced with 60 µL Calcium Assay Buffer. Cells were maintained at room temperature for the assay. For calcium fluorescence measurement of antagonist potency, antagonist concentration-response curves (20 µL, 5X) were added 20 s after the beginning of data collection and an EC_{80} concentration of agonist (20 µL, 5X) was added 90 s later via a Flexstation II (Molecular Devices, Sunnyvale, CA). Fluorescence imaging continued for a total of 160 s acquisition time using an excitation of 488 nm, an emission of 525 nm, and a cutoff of 515 nm. Agonist and antagonist were added at a speed of 52 µl/s, and calcium flux was measured using a Flexstation II at 25°C. For Schild analyses, fixed concentrations of antagonist were added manually (20 µL, 5X) so that the agonist concentration-response curve was added via a Flexstation II following a 15 min incubation with antagonist. All of the peaks of the calcium response were normalized to the response to a maximally effective concentration of ACh (ECMax). The concentration of ACh that elicited a response that is 80% of max (EC_{80} value) was determined for every separate experiment, allowing for a response varying from 70 to 90% of the maximum peak. These maximum values were fit using GraphPad Prism version 4.0 to a 4 parameter logistic equation to determine IC_{50} values and Schild Dose-Ratios.

Hippocampal Phosphoinositide (PI) hydrolysis. PI hydrolysis in hippocampal slices was measured as previously described (Conn and Sanders-Bush, 1986) with a few modifications. Briefly, Cross-chopped (350 µM X 350 µM) slices of male (6-9 weeks) Sprague-Dawley rat hippocampus were incubated with 95% O_2 / 5% CO_2 bubbled Krebs buffer (108 mM NaCl, 4.7

Downloaded from molpharm.aspetjournals.org at ASPET Journals on April 20, 2024

Molecular Pharmacology Fast Forward. Published on April 30, 2009 as DOI: 10.1124/mol.109.056531
This article has not been copyedited and formatted. The final version may differ from this version.

mM KCl, 1.2 mM $MgSO_4$, 1.2 mM KH_2PO_4, 2.5 mM $CaCl_2$, 25 mM $NaHCO_3$ and 10 mM Glucose). The tissue was allowed to recover for 30 min with shaking at 37^{o}C. Following tissue recovery, the tissue was combined, washed with warm Krebs buffer, and 25 µL of gravity packed slices were incubated with 175 µL Krebs containing 0.5 µCi [^{3}H]myo-inositol (Perkin-Elmer, Waltham, MA) for 45 min. VU0255035 or vehicle controls were added and incubated for 15 min, followed by the addition of 10 mM LiCl and incubation for an additional 15 min. Finally, an EC_{80} concentration of carbachol (CCh) was added, followed by an additional 45 min incubation. The reaction was terminated by the addition of 900 µL of chloroform:methanol (1:2). The aqueous and organic phases were separated by addition of 300 µL chloroform and 300 µL water, vortexing, and allowing the phases to separate by gravity. The aqueous phase was added to anion exchange columns (AG 1-X8 Resin, 100-200 mesh, formate form, BIO-RAD, Hercules, CA) and [^{3}H]inositol phosphates were eluted and measured by liquid scintillation counting. Data were fit with GraphPad Prism version 4.0 to a 4 parameter logistic equation to determine IC_{50} values.

Membrane preparation and Equilibrium Radioligand Binding. Membranes were prepared and equilibrium radioligand binding assays were performed as has been previously described (Shirey et al., 2008).

Electrophysiology. Transverse hippocampal slices were prepared from Sprague-Dawley rats (postnatal day 17-25). Rats were anesthetized with isoflurane and decapitated. The brain was rapidly removed from the skull and submerged in ice-cold modified artificial cerebrospinal fluid (ACSF), which was oxygenated with 95% O_2 / 5% CO_2 and composed of (in mM) 230 sucrose,

Downloaded from molpharm.aspetjournals.org at ASPET Journals on April 20, 2024

Molecular Pharmacology Fast Forward. Published on April 30, 2009 as DOI: 10.1124/mol.109.056531
This article has not been copyedited and formatted. The final version may differ from this version.

2.5 KCl, 0.5 $CaCl_2$, 6 $MgSO_4$, 1.25 NaH_2PO_4, 26 $NaHCO_3$, and 10 D-glucose. The brain was blocked in the horizontal plane, glued to the stage of a vibratome (Vibratome, St. Louis, MO) that was filled with ice-cold modified ACSF, and cut at 290 μm. Slices were then incubated in oxygenated normal ACSF (in mM, 126 NaCl, 2.5 KCl, 3 $CaCl_2$, 1 $MgSO_4$, 1.25 NaH_2PO_4, 26 $NaHCO_3$, and 10 D-glucose) at 31-32°C for 30 min and maintained at room temperature afterward until transferred individually to a fully submerged recording chamber, which was continuously perfused with oxygenated ACSF at ~30°C.

Whole-cell recordings were made from visually identified hippocampal CA1 pyramidal neuron soma under an Olympus BX50WI upright microscope (Olympus, Lake Success, NY). A low-power objective (4x) was used to identify CA1 region of the hippocampus, and a 40x water immersion objective coupled with Hoffman optics and video system was used to visualize individual pyramidal cells. A MultiClamp 700B amplifier (Molecular devices, Union City, CA) was used for voltage-clamp recordings. Patch pipettes (4-6 MΩ) were prepared from borosilicate glass (World Precision Instrument, Sarasota, FL) using a Narashige vertical patch pipette puller (Narashige, Japan) and filled with the pipette solution containing (in mM) 61.5 K-gluconate, 65 CsCl, 3.5 KCl, 1 $MgCl_2$, 0.5 $CaCl_2$, 10 HEPES, 5 EGTA, 2 Mg-ATP, and 0.2 Na-GTP. The pH of the pipette solution was adjusted to 7.3 with 1 M KOH, and osmolality was adjusted to ~295 mOsm/kg. Cells were voltage-clamped at -60 mV and NMDA receptor mediated currents were induced by pressure ejection of 1 mM NMDA to the soma of the recorded cell through a patch pipette using a Picospritzer II (General Valve, Fairfield, NJ). The experiment was carried out in the presence of tetrodotoxin (1 μM) to block voltage-gated sodium channels. All drugs were bath applied. Data acquisition and analysis were performed using a PC computer equipped with pCLAMP software (Molecular Devices, Union City, CA). Data are presented as percentage of

Downloaded from molpharm.aspetjournals.org at ASPET Journals on April 20, 2024

Molecular Pharmacology Fast Forward. Published on April 30, 2009 as DOI: 10.1124/mol.109.056531
This article has not been copyedited and formatted. The final version may differ from this version.

the control value or percentage potentiation. The percent potentiation was defined by [I(max)/I(control)-1]x100, where I(control) was the average amplitude of NMDA receptor currents of 4 trials immediately before application of CCh or VU0255035 and I(max) is the maximum current amplitude during drug application. Statistical analysis of electrophysiology data was performed using two-tailed paired or unpaired Student's *t*-test as appropriated and p-values less than 0.05 ($p < 0.05$) were considered to be significant. Data are presented as mean ± S.E.M.

Animals. Experiments were conducted in accordance with the US National Institutes of Health regulations of animal care and approved by the Institutional Animal Care and Use Committee, Vanderbilt University Medical Center. Subjects were housed in groups of two to four per cage in a large colony room under a 12-h light-dark cycle (lights on at 6:00 a.m.) with food and water provided *ad libitum.*

Pilocarpine-Induced Seizures. Hybrid mice (C57Bk:129Sv; 2-6 months old) were used for these studies. The susceptibility of these mice to pilocarpine-induced seizures was assessed with a single intraperitoneal (i.p.) injection of pilocarpine (280 mg/kg). VU0255035 was prepared in 5% lactic acid, diluted to 10 mM with H_2O, and the pH was adjusted to 6.5 – 7.0 using 1N NaOH. The 10 mM VU0255035 stock was then filtered using a 0.2 micron filter and diluted to a 2 mM stock with 9% saline. Each mouse was first injected with methylscopolamine nitrate (1 mg/kg; i.p.) to block the peripheral effects of pilocarpine. Immediately thereafter, each mouse was injected i.p. with either vehicle or VU0255035 (10 mg/kg), followed 30 minutes later with an i.p. injection of pilocarpine (280 mg/kg). Seizures induced by pilocarpine were recorded by a

Downloaded from molpharm.aspetjournals.org at ASPET Journals on April 20, 2024

Molecular Pharmacology Fast Forward. Published on April 30, 2009 as DOI: 10.1124/mol.109.056531
This article has not been copyedited and formatted. The final version may differ from this version.

digital camcorder and scored at a later time for each 5-min period. The scoring was based on the modified Racine scale, as described at the following stages: 0, no abnormality; 1, exploring, sniffing, and grooming ceased, becoming motionless; 2, forelimb and/or tail extension, appearance of rigid posture; 3, myoclonic jerks of the head and neck, with brief twitching movement, or repetitive movements with head bobbing or "wet-dog shakes"; 4, forelimb clonus and partial rearing, or occasional rearing and falling; 5, forelimb clonus, continuous rearing and falling; 6, tonic-clonic movements with loss of posture tone, often resulting in death. The seizure scores for the first 45 min after pilocarpine injection for the control group and VU0255035 treated group were analyzed using 2-way ANOVA.

Pharmacokinetic analysis. Male Sprague-Dawley rats (Harlan, Indianapolis, IN) weighing approximately 250 g were used for the pharmacokinetics (PK) studies. VU0255035 was administered i.p. at a dose of 10 mg/kg. The dosing solution was prepared in 5% lactic acid (8.5% v/v) in water and the pH was adjusted to 6.5 using 1N NaOH. Blood and brain tissue samples were collected at 0.5, 1, 2, 4, and 8 h post dose. The blood samples were collected by cardiac puncture and processed to separate plasma. The animals were decapitated to collect the whole brain tissue samples. Both plasma and brain tissues were immediately frozen in dry ice and stored in -80 °C until analysis. Before analysis, the brain samples were washed to remove residual blood, weighed, and homogenized in 5 ml of phosphate buffered saline using ultrasonic homogenizer. The plasma and brain homogenate samples were processed by acetonitrile precipitation method and analyzed using LC-MS-MS. The LC separation was carried out on a Luna ODS column (5 µm, 2.1 mm × 5 cm; Phenomenex, Torrance, CA) at a flow rate of 0.3 ml/min. The gradient program was used with the mobile phase, combining solvent A (95: 5:

Downloaded from molpharm.aspetjournals.org at ASPET Journals on April 20, 2024

Molecular Pharmacology Fast Forward. Published on April 30, 2009 as DOI: 10.1124/mol.109.056531
This article has not been copyedited and formatted. The final version may differ from this version.

0.1% formic acid in water: acetonitrile) and solvent B (95: 5: acetonitrile: 0.1% formic acid in water) as follows: 0% B for 0-2 min, 0–100% B for 2-2.5 min, 100% B for 2.5-3.5 min, 100–0% B for 3.5- 4.0 min and finally equilibration for 2 min before injection of next sample. Mass spectrometry was carried out using a ThermoFinnigan TSQ Quantum Ultra (Thermo Fisher Scientific, Waltham, MA) mass spectrometer in positive ion mode. The software Xcalibur version 2.0 was used to control the instrument and collect data. The electrospray ionization source was fitted with a stainless steel capillary (100 µm i.d.). Nitrogen was used as both the sheath gas and the auxiliary gas. The ion transfer tube temperature was 300°C. The spray voltage, tube lens voltage, and pressure of sheath gas and auxiliary gas were optimized to achieve maximal response using the test compounds mixing with the mobile phase A (50%) and B (50%) at a flow rate of 0.3 ml/min. Collision-induced dissociation was performed on the VU0255035 and internal standard (VU178) under 1.0 mTorr of argon. Selected reaction monitoring was carried out using the transitions *m*/*z* 433 to 164 for VU0255035, and *m*/*z* 310 to 223 for internal standard (VU178). The calibration curves were constructed and linear response was obtained in the range of 1- 500 ng/ml by spiking known amounts of analytes in blank brain homogenates and plasma. The concentrations were expressed as ng/ml or ng/g of tissue. The concentration-time data was analyzed by noncompartmental analysis using WinNonlin 5.2 (Pharsight Inc.)

Contextual Fear Conditioning. Contextual fear conditioning studies were conducted in conditioning chambers housed in a sound-attenuating cubicle (Med Associates, St. Albans, VT) with a fluorescent light mounted on the back wall of the cubicle to provide illumination for the chamber. Stainless steel grid floors connected to shock scramblers and generators delivered the

Downloaded from molpharm.aspetjournals.org at ASPET Journals on April 20, 2024

Molecular Pharmacology Fast Forward. Published on April 30, 2009 as DOI: 10.1124/mol.109.056531
This article has not been copyedited and formatted. The final version may differ from this version.

0.5 mA unconditioned stimulus. A digital video camera mounted on the front wall of the cubicle was interfaced with a PC equipped with Video Freeze software (MED-VFC-RS, Med Associates), which incorporated a pixel-based method to measure and quantify freezing behavior. Based on previous studies, the motion threshold was set at 120 arbitrary units, 5-second freeze duration. All trials were recorded at 30 frames per second. In addition, 1 mL of a 10% vanilla extract solution was applied to the conditioning chamber grid floor to provide an olfactory cue.

Male Sprague-Dawley rats (Harlan, Indianapolis, IN.), weighing 240-270 g, were handled and injected with vehicle for two days prior to training. On training day, rats were habituated for 30 min in the training room. For the scopolamine dose-response studies, rats were pretreated for 15 min s.c. with either vehicle (0.9% saline) or a dose of scopolamine (0.03-0.3 mg/kg) prior to the training session. Based on the PK studies with VU0255035, rats were pretreated for 30 min i.p. with either vehicle (5% lactic acid (8.5% v/v) in water, pH adjusted to 6.5 using 1N NaOH) or a dose of VU0255035 (3-30 mg/kg) prior to the training session. During the training session, rats were then placed in the conditioning chamber. Rats were then given a 2 min habituation, followed by 4 tone/shock pairing trials. The tone (30 s, 5 kHz, 70 dB) presented through a speaker initiated each trial and coterminated with an electric foot-shock (1 s, .5 mA). A 45 s intertrial interval (ITI) separated each tone/shock pairing trials. After the fourth and final tone/shock pairing, the rat remained in the chamber for an additional 45 s without tone or shock stimuli. All rats received the same conditioned freezing training protocol.

Approximately 24 h after training, the magnitude of contextual fear conditioning response was tested by placing the rats back into the same conditioning chambers with identical visual and odor cues and measuring freezing behavior in the absence of any auditory or shock

Downloaded from molpharm.aspetjournals.org at ASPET Journals on April 20, 2024

Molecular Pharmacology Fast Forward. Published on April 30, 2009 as DOI: 10.1124/mol.109.056531
This article has not been copyedited and formatted. The final version may differ from this version.

stimuli for an 7 min period equivalent to the duration of the training session. Memory of the fear response post-24 h after training was assessed by recording the amount of freezing response in the testing chamber environment. Freezing was defined as a motionless posture, except for respiratory movements and calculated as the percent of freezing behavior for the entire testing session. Data were analyzed using a one-way analysis of variance and if significant ($p<0.05$), all dose groups were compared to the vehicle group using a Dunnett's test.

Medicinal Chemistry Methods

General. All NMR spectra were recorded on a Bruker 400 MHz instrument. ^{1}H chemical shifts are reported in δ values in ppm downfield from DMSO as the internal standard in DMSO. Data are reported as follows: chemical shift, multiplicity (s = singlet, d = doublet, t = triplet, q = quartet, br = broad, m = multiplet), integration, coupling constant (Hz). ^{13}C chemical shifts are reported in δ values in ppm with the DMSO carbon peak set to 39.5 ppm. Low resolution mass spectra were obtained on an Agilent 1200 series 6130 mass spectrometer with electrospray ionization. High resolution mass spectra were recorded on a Waters Q-TOF API-US. Analytical thin layer chromatography was performed on Analtech silica gel GF 250 micron plates. Analytical HPLC was performed on an Agilent 1200 series with UV detection at 214 nm and 254 nm along with ELSD detection. Preparative purification was performed on an ISCO combi-flash companion. Solvents for extraction, washing and chromatography were HPLC grade. All reagents were purchased from Aldrich Chemical Co. and were used without purification. All polymer-supported reagents were purchased from Biotage, Inc.

Downloaded from molpharm.aspetjournals.org at ASPET Journals on April 20, 2024

Molecular Pharmacology Fast Forward. Published on April 30, 2009 as DOI: 10.1124/mol.109.056531
This article has not been copyedited and formatted. The final version may differ from this version.

Standard Experimental Procedures for Key Compounds

Methyl 3-(benzo[*c*][1,2,5]thiadiazole-4-sulfonamido)propanoate (2). To a solution of β-alanine methyl ester (2.36 g, 17.0 mmol) in CH_2Cl_2 (70 mL) was added DIPEA (6.56 mL, 37.4 mmol) and 2,1,3-benzothiadiazole-4-sulfonyl chloride (4.01 g, 17.0 mmol). The reaction was stirred at room temperature for 20 h. The reaction was partially concentrated under vacuum and purified by column chromatography (silica gel) using 0 to 55 % EtOAc in hexanes to afford a crude orange solid. Triturated with CH_2Cl_2/hexanes (1:2, 70 mL) to afford **2** as a pale yellow solid (3.81 g, 74%): mp 119.6-119.9 °C; ^{1}H NMR (400 MHz, DMSO-d_6) δ 8.38 (dd, *J* = 9.0, 1.0 Hz, 1H), 8.19 (dd, *J* = 7.0, 1.0 Hz, 1H), 7.94 (t, *J* = 6.0 Hz, 1H), 7.85 (dd, *J* = 9.0, 7.0 Hz, 1H), 3.44 (s, 3H), 3.19 (q, *J* = 6.5 Hz, 2H), 2.46 (t, *J* = 6.5 Hz, 2H); ^{13}C NMR (100 MHz, DMSO-d_6) δ 171.5, 155.4, 149.1, 132.6, 130.9, 129.3, 126.4, 51.6, 39.03, 34.5; Analytical LCMS (J-Sphere80-C18, 3.0 x 50.0 mm, 4.1 min gradient, 5%[0.05% TFA/CH_3CN]:95%[0.05% TFA/H_2O]: 2.31 min, >99%, (214 nM, 254 nm, ELSD), m/z [M+Na] = 324.0; HRMS calc'd for $C_{10}H_{12}N_3O_4S_2$ [M+H]; 302.0305 found 302.0269.

3-(benzo[*c*][1,2,5]thiadiazole-4-sulfonamido)propanoic acid (3). To a solution of methyl ester **2** (3.70 g, 12.2 mmol) in THF (45 mL) was added MeOH (10 mL) and 2N NaOH (10 mL). The reaction was stirred at room temperature for 4h. Quenched upon addition of 2 N HCl (45 mL) and extracted with EtOAc (2 x 100 mL). The combined organic extracts were dried over $MgSO_4$, concentrated under vacuum and triturated with CH_2Cl_2/hexanes (1:1, 70 mL) to afford acid **3** as an off-white solid (2.54g, 72%); mp 176.1-176.3 °C; ^{1}H NMR (400 MHz, DMSO-d_6) δ 8.37 (dd, *J* = 9.0, 1.0 Hz, 1H), 8.19 (dd, *J* = 7.0, 1.0 Hz, 1H), 7.92-7.79 (m, 2H), 3.33 (br s, 1H), 3.15 (q, *J*

Downloaded from molpharm.aspetjournals.org at ASPET Journals on April 20, 2024

Molecular Pharmacology Fast Forward. Published on April 30, 2009 as DOI: 10.1124/mol.109.056531
This article has not been copyedited and formatted. The final version may differ from this version.

= 7.0 Hz, 2H), 2.32 (t, *J* = 7.0 Hz, 2H); ^{13}C NMR (100 MHz, DMSO-d_6) δ 172.6, 155.4, 149.2, 132.6, 130.9, 129.3, 126.4, 39.1, 34.6; Analytical LCMS (J-Sphere80-C18, 3.0 x 50.0 mm, 4.1 min gradient, 5%[0.05% TFA/CH_3CN]:95%[0.05% TFA/H_2O]: 1.99 min, >99%, (214 nM, 254 nm, ELSD),m/z [M+Na] = 310.0; HRMS calc'd for $C_9H_{10}N_3O_4S_2$ [M+H]; 288.0113 found 288.0110.

General Library Synthesis Protocol. To a solution of acid **3** (50 mg, 0.17 mmol) and DIPEA (46 μL, 0.34 mmol) in DCM (2 mL) in a 4-mL vial was added polymer-supported DCC (283 mg, 0.34 mmol, 1.2 mmol/g), HOBt (27 mg, 0.2 mmol) and one of 24 amines (HNR_1R_2) and rotated at room temperature for 20 h. Then, MP-carbonate (151 mg, 0.5 mmol, 3.3 mmol/g) was added to scavenge excess **3** and the HOBt. The reactions were filtered into 13 x 100 mm test tubes, and the resin washed (3 x 5 mL) with DCM. The combined organic layers were dried down on a nitrogen evaporator and the compounds purified to >98% by preparative LCMS on an Agilent 1200 Prep mass-directed LCMS purification system.

***N*-(3-oxo-3-(4-(pyridine-4-yl)piperazin-1-yl)propyl)benzo[c][1,2,5]thiadiazole-4 sulfonamide (5b, VU0255035).** To a solution of acid **3** (2.00 g, 6.94 mmol) and DIPEA (2.43 mL, 13.9 mmol) in DMF (10 mL) was added EDC (1.55 g, 8.33 mmol), HOBt (937 mg, 6.94 mmol) and 1-(4-pyridyl)piperazine (1.36 g, 8.33 mmol) and stirred at room temperature for 20 h. The reaction was diluted with water (80 mL) and extracted with EtOAc (2 x 100 mL). The combined organic extracts were washed with water (2 x 80 mL) and brine (100 mL), dried over $MgSO_4$ and concentrated under vacuum. The residue was triturated with CH_2Cl_2/hexanes (1:1, 40 mL) to afford amide **VU0255035 (5b)** as a light tan solid (1.45 g, 48 %): mp 159.7-160.2 °C;

Downloaded from molpharm.aspetjournals.org at ASPET Journals on April 20, 2024

Molecular Pharmacology Fast Forward. Published on April 30, 2009 as DOI: 10.1124/mol.109.056531
This article has not been copyedited and formatted. The final version may differ from this version.

^{1}H NMR (400 MHz, DMSO-d_6) δ 8.37 (d, *J* = 9.0 Hz, 1H), 8.20 (d, *J* = 7.0 Hz, 1H), 8.16 (d, *J* = 6.0 Hz, 2H), 7.85 (dd, *J* = 9.0, 7.0 Hz, 1H), 7.71 (br s, 1H), 6.80 (d, *J* = 6.0 Hz, 2H), 3.51-3.40 (m, 4H), 3.35-3.28 (m, 4H), 3.21-3.12 (m, 2H); ^{13}C NMR (100 MHz, DMSO-d_6) δ 169.1, 155.4, 154.7, 149.5, 149.2, 132.5, 130.9, 129.3, 126.3, 108.6, 45.6, 45.3, 44.2, 41.7, 41.4, 33.0; Analytical LCMS (J-Sphere80-C18, 3.0 x 50.0 mm, 4.1 min gradient, 5%[0.05% TFA/CH_3CN]:95%[0.05% TFA/H_2O]: 1.95 min, >99%, (214 nM, 254 nm, ELSD), m/z [M+H] = 433.1; HRMS calc'd for $C_{18}H_{21}N_6O_3S_2$ [M+H]; 433.1117 found 433.1117.

Downloaded from molpharm.aspetjournals.org at ASPET Journals on April 20, 2024

Molecular Pharmacology Fast Forward. Published on April 30, 2009 as DOI: 10.1124/mol.109.056531
This article has not been copyedited and formatted. The final version may differ from this version.

Results

Identification of novel M_1 antagonists using a high-throughput screening (HTS) approach.

To search for novel antagonists of M_1, we initiated a high-throughput screen of a small molecule library within the Vanderbilt screening and chemistry center of the NIH Molecular Libraries Screening Center Network (MLSCN) (http://www.vanderbilt.edu/mlscn/Templates/index.htm) (Lewis et al., 2008). A small molecule library of 63,656 compounds from the MLSCN collection was screened against CHO cells expressing the rM_1 mAChR by utilizing a real-time cell-based calcium-mobilization assay (Z' averaged 0.7). This effort identified 2,179 primary M_1 antagonist hits, of which 1,665 compounds were available from Biofocus-DPI for re-test. Following re-tests, 723 hits were confirmed, demonstrating a 43% re-test rate. To eliminate compounds that may inhibit calcium mobilization responses by a mechanism that is not specific to mAChR activation, the 723 verified hits were counter-screened against a CHO cell line expressing the metabotropic glutamate receptor 4 (mGluR4) and the chimeric G protein G_{qi5}. This secondary screen eliminated 9 of the original hits. The remaining hits were tested in triplicate as 10-point concentration response curves (CRCs) against both rM_1 CHO cells and a CHO cell line expressing rM_4 and the chimeric G protein G_{qi5} to identify compounds selective for M_1 versus M_4 mAChRs. The majority of compounds displayed no subtype selectivity. However, compound 1 (**Figure 1, inset**), based on a N-(3-piperazin-1-yl)-3-oxopropyl)benzo[c][1,2,5]thiadiazole-4-sulfonamide scaffold, was selective for M_1 versus M_4 mAChRs. Compound 1 inhibited a submaximal (EC_{80}) concentration of ACh at M_1 with an IC_{50} of 2.4 $\pm$ 1.2 μM (**Figure 1**). In contrast, compound 1 did not induce robust inhibition of an EC_{80} of ACh at M_4 mAChRs (IC_{50} of

Downloaded from molpharm.aspetjournals.org at ASPET Journals on April 20, 2024

Molecular Pharmacology Fast Forward. Published on April 30, 2009 as DOI: 10.1124/mol.109.056531
This article has not been copyedited and formatted. The final version may differ from this version.

> 150 μM), demonstrating a greater than 60-fold selectivity for M_1 versus M_4 mAChRs. Although this was promising, Compound 1 had relatively low potency at inhibiting M_1. Thus, we initiated a chemical lead optimization effort to improve M_1 potency while maintaining selectivity.

Chemical Optimization of HTS Lead 1.

For chemical optimization of HTS lead **1**, analogues of **1** were synthesized in a library format according to **Supplemental Figure 1**. For our initial efforts, we explored alternative amides in place of the 2-pyridylpiperizine moiety. The synthesis began by treating commercially available benzo[*c*]thiadiazole-4-sulfonyl chloride (**2**) with β-alanine methyl ester under standard amide coupling conditions to afford, after saponification with LiOH/THF/MeOH/H_2O, the acid (**3**) in 55% yield for the two steps. Subsequent coupling with a diverse collection of amines under standard solution phase parallel synthesis conditions employing polymer-supported reagents and scavengers provided 24 analogues (**4**) (Kennedy et al., 2008). All analogs were purified by mass-directed HPLC to analytical purity (Leister et al., 2003).

Chemically Optimized Compounds are Potent and Selective M_1 mAChR Antagonists.

This library of compounds was initially evaluated for activity at inhibiting the response of M_1 to an EC_{80} concentration of ACh. The structure activity relationship (SAR) for this series was relatively flat with functionalized piperazine amides represented by structure **5** being the only active congeners of structure **4** (**Figure 2A**). As shown in **Figure 2B**, a simple phenyl piperazine analog **5c** (IC_{50} > 10 μM), was nearly inactive at M_1, relative to compound **1**. Functionalized phenyl piperazine analogues, such as the 3-OMePh congener **5e** (IC_{50} > 10 μM) and the 2-CNPh

Downloaded from molpharm.aspetjournals.org at ASPET Journals on April 20, 2024

Molecular Pharmacology Fast Forward. Published on April 30, 2009 as DOI: 10.1124/mol.109.056531
This article has not been copyedited and formatted. The final version may differ from this version.

derivative **5f** (IC_{50} > 10 μM) also demonstrated limited M_1 mAChR activity. In addition, aliphatic piperazine analogues, such as i-Pr **5h** (IC_{50} > 10 μM), were devoid of any mAChR antagonist activity. Piperazinyl pyridine isomers proved to be the most interesting analogs. Relative to the 2-pyridyl analog compound **1**, the 3-pyridyl congener, **5a** (IC_{50} = 3.2 ± 1.6 μM), possessed roughly equivalent activity at M_1, while also maintaining selectivity versus M_2-M_5 (data not shown). The 4-pyridyl variant, **5b** (IC_{50} = 309.1 ± 100.5 nM), provided an ~8-fold increase in M_1 potency relative to the HTS hit **1**. Compound **5b** was resynthesized on a gram scale, renamed VU0255035, and further evaluated.

The next critical step was to confirm that VU0255035 maintains mAChR subtype selectivity. The potency of VU0255035 for inhibition of an EC_{80} ACh response was determined for M_1-M_5 mAChRs (**Figure 3**). VU0255035 induced only weak inhibition of M_2, M_3, M_4, and M_5 responses to ACh with IC_{50} values > 10 μM at each subtype. Thus, VU0255035 had an IC_{50} of 132.6 ± 28.5 nM at M_1 upon retest of the resynthesized compound and exhibited a 75-fold or greater functional selectivity for the M_1 mAChR relative to other mAChR subtypes. VU0255035 has greater functional selectivity than any previous small molecule M_1 antagonist and rivals the mAChR selectivity profile of the MT7 snake venom toxin (Karlsson et al., 2000).

VU0255035 is a competitive antagonist of M_1 mAChRs.

In previous efforts, we and others have had great success in achieving high subtype selectivity for mAChR activators by targeting allosteric sites rather than the orthosteric ACh binding site (Conn et al., 2009). To determine whether VU0255035 binds to the orthosteric binding site, we performed equilibrium radioligand binding studies. Membranes prepared from CHO cells expressing M_1-M_5 mAChRs were incubated with a 0.1 nM of the orthosteric site

Downloaded from molpharm.aspetjournals.org at ASPET Journals on April 20, 2024

Molecular Pharmacology Fast Forward. Published on April 30, 2009 as DOI: 10.1124/mol.109.056531
This article has not been copyedited and formatted. The final version may differ from this version.

antagonist l-[N-methyl-^{3}H]scopolamine ([^{3}H]-NMS) in the absence or presence of increasing concentrations of either atropine (Messer, 2002) or VU0255035. This concentration of [^{3}H]-NMS is non-saturating (Shirey et al., 2008) and all specific binding data represent less than 10% of the total binding. Atropine displaced [^{3}H]-NMS binding in membranes from cells expressing each of the mAChR subtypes with high affinity, displaying no subtype selectivity, consistent with what has been previously reported (**Figure 4B and Table 1**) (Bymaster and Falcone, 2000). VU0255035 also displaced [^{3}H]-NMS binding from membranes expressing each of the mAChR subtypes (**Figure 4A**). However, in contrast to atropine, VU0255035 had a much higher affinity for the orthosteric site of M_1 mAChRs than for M_2-M_5, showing greater than a 45-fold selectivity relative to M_2 and even greater selectivity for M_1 relative to the other mAChR subtypes (**Table 1**).

We then performed saturation binding experiments with increasing concentrations of [^{3}H]-NMS in the absence or presence of 10 nM, 30 nM, or 100 nM VU0255035. Scatchard analysis was performed (**Figure 5**) to determine whether VU0255035 reduces [^{3}H]-NMS binding in a manner that is consistent with competitive interaction with the [^{3}H]-NMS binding site. Nonspecific binding was determined in the presence of 1 μM atropine. Scatchard analysis revealed data consistent with binding of [^{3}H]-NMS to a single site in the absence of antagonist (linear regression, $r^2 = 0.99$). The K_d value of [^{3}H]-NMS in the absence of antagonist was 0.17 nM, consistent with previous studies (Shirey et al., 2008). Increasing concentrations of VU0255035 maintained a linear Scatchard regression line (linear regression, $r^2 = 0.99$ for 10 nM VU0255035, $r^2 = 0.98$ for 30 nM VU0255035, $r^2 = 0.99$ for 100 nM VU0255035) and had no effect on the predicted receptor density (B_{max}) but altered the slope of the regression line (**Figure 5**). The apparent affinity of [^{3}H]-NMS was reduced by VU0255035, with K_d values of 0.25 nM,

Downloaded from molpharm.aspetjournals.org at ASPET Journals on April 20, 2024

Molecular Pharmacology Fast Forward. Published on April 30, 2009 as DOI: 10.1124/mol.109.056531
This article has not been copyedited and formatted. The final version may differ from this version.

0.37 nM, or 0.76 nM for 10 nM, 30 nM, or 100 nM VU0255035 respectively. The reduction in apparent K_d with no accompanying change in linearity of the regression line or the apparent B_{max} is consistent with a competitive interaction of VU0255035 with the [^{3}H]-NMS binding site.

We further evaluated the question of whether VU0255035 inhibits M_1 mAChRs by a competitive or noncompetitive mechanism in functional studies by performing a Schild analysis. Concentration-response relationships of ACh-induced increases in calcium mobilization in the absence or presence of increasing concentrations of VU0255035 (100 nM, 300 nM, 1 μM, 3 μM) (**Figure 6A**) were evaluated. The maximum response to ACh was not significantly altered by increasing concentrations of VU0255035, but VU0255035 induced parallel rightward shifts in the ACh concentration response relationships. Analysis of the data using a Schild analysis (Arunlakshana and Schild, 1959) (**Figure 6B**) revealed a Schild regression line with a slope that was not statistically different from unity (linear regression slope = 0.95 ± 0.16) and a calculated K_d of 33 nM for VU0255035. These data are consistent with a competitive interaction of VU0255035 with the orthosteric ACh site. We also performed a Schild analysis of the effect of VU0255035 on the response of M_1 to TBPB, an allosteric agonist of M_1 (Jones et al., 2008). In contrast with the Schild analysis using ACh, Schild analysis of effects of VU0255035 on the response to TBPB revealed a Schild regression slope statistically different from unity (linear regression slope = 0.69 ± 0.06) (**Figure 6B**). These data are consistent with the hypothesis that VU0255035 does not interact with the same site as the allosteric agonist TBPB and that VU0255035 is acting as a competitive orthosteric site antagonist.

To further validate that VU0255035 is acting as an orthosteric antagonist, we determined the effect of VU0255035 on a mutant version of the M_1 muscarinic receptor containing a point mutation that renders the receptor less sensitive to acetylcholine or orthosteric antagonists (Jones

Downloaded from molpharm.aspetjournals.org at ASPET Journals on April 20, 2024

Molecular Pharmacology Fast Forward. Published on April 30, 2009 as DOI: 10.1124/mol.109.056531
This article has not been copyedited and formatted. The final version may differ from this version.

et al., 2008; Spalding et al., 2006). Mutation of tyrosine 381 to alanine (Y381A) in the M_1 mAChR causes a large rightward shift in the potency of the orthosteric agonist ACh. The EC_{50}s for ACh were 2.5 ± 0.3 nM for wildtype M_1 (WT) versus 13.7 ± 1.6 μM for the Y381A mutant (Y381A) (**Figure 7A**). In contrast to ACh, the potency of an allosteric agonist of the M_1 mAChR, N-desmethylclozapine (NDMC) (Sur et al., 2003), is unaffected by the Y381A mutation. The EC_{50} values for NDMC were 140.5 ± 26.1 nM for WT versus 162.4 ± 6.1 nM for Y381A (**Figure 7A**). If VU0255035 acts as a competitive orthosteric site antagonist, its potency should be decreased by the Y381A mutation. Consistent with this, VU0255035 potency was dramatically reduced in cells expressing M_1-Y381A when compared with cells expressing WT M_1 (**Figure 7B**). The IC_{50} values for VU0255035 versus ACh were 53.3 ± 7.7 nM for WT versus 38.9 ± 0.2 μM for Y381A, demonstrating greater than a 500-fold right shift in potency versus ACh. The IC_{50} values for VU0255035 versus NDMC were 57.3 ± 3.5 nM for WT versus 33.4 ± 8.4 μM for Y381A, also demonstrating greater than a 500-fold right shift in potency versus NDMC. Together, these data demonstrate that Y381A mutation equivalently impacts VU0255035 potency, whether measured versus ACh or NDMC. These data are consistent with the data from radioligand binding and Schild analysis studies and indicate that VU0255035 is acting as a competitive orthosteric M_1 mAChR antagonist.

VU0255035 inhibits carbachol-induced increases in PI hydrolysis in rat hippocampal slices.

To verify that VU0255035 can block M_1-mediated responses in native tissue preparations, we determined effects of this compound on activation of phosphoinositide (PI) hydrolysis by mAChR agonists in hippocampal slices. The PI hydrolysis responses to non-selective mAChR agonists, such as carbachol (CCh), are nearly abolished in M_1 knockout mice,

Downloaded from molpharm.aspetjournals.org at ASPET Journals on April 20, 2024

Molecular Pharmacology Fast Forward. Published on April 30, 2009 as DOI: 10.1124/mol.109.056531
This article has not been copyedited and formatted. The final version may differ from this version.

suggesting that this response is mediated by M_1 mAChRs (Porter et al., 2002). We performed initial studies measuring PI hydrolysis in rat hippocampal slices with a range of concentrations of CCh to determine a submaximal concentration of CCh (EC_{80}) to utilize (data not shown). VU0255035 blocked the PI hydrolysis response to an EC_{80} concentration of CCh in rat hippocampal slices in a concentration-dependent manner (**Figure 8**) with an IC_{50} value of 2.4 ± 1.0 μM.

VU0255035 inhibits CCh-induced potentiation of NMDA receptor currents in hippocampal CA1 pyramidal cells.

Activation of mAChRs in hippocampal pyramidal cells and in other brain regions has been demonstrated to result in the potentiation of NMDA receptor-mediated currents and the mAChR-mediated potentiation of NMDA currents in CA1 pyramidal cells in the hippocampus has been demonstrated to be mediated by activation of M_1 mAChRs (Marino et al., 1998; Rouse et al., 1999). Thus, we determined the effect of VU0255035 on NMDA receptor (NMDAR)-mediated inward currents in CA1 pyramidal cells. Cells were voltage-clamped at -60 mV and NMDA receptor currents (I_{NMDA}) were evoked by pressure ejection of NMDA (1 mM) applied in the region of the cell soma. As has been previously shown (Marino et al., 1998), bath application of the cholinergic agonist CCh (10 μM) induced an increase in the peak amplitude of NMDA-evoked currents in pyramidal cells (**Figure 9A**). The increased amplitude of NMDAR currents peaked at 163.6 ± 17.1 % of baseline (n = 9, p = 0.0072) approximately 2 min after initial application of CCh and decayed rapidly. To determine if VU0255035 could antagonize the CCh effect of potentiating NMDAR currents, we bath applied VU0255035 (5 μM) prior to the application of CCh. As illustrated in **Figure 9B** and summarized in **Figure 9C**, VU0255035 (5

Downloaded from molpharm.aspetjournals.org at ASPET Journals on April 20, 2024

Molecular Pharmacology Fast Forward. Published on April 30, 2009 as DOI: 10.1124/mol.109.056531
This article has not been copyedited and formatted. The final version may differ from this version.

μM) completely blocked the CCh-induced potentiation of NMDAR currents with a peak potentiation of 10.3 ± 7.7% in the presence of VU0255035 (n = 7) as compared to a peak potentiation of 63.6 ± 17.1% observed in control (n = 9; p = 0.016), consistent with VU0255035 antagonizing M_1 mAChRs. VU0255035 by itself had no significant effect on NMDAR currents (107.4 ± 8.5 % of baseline, n = 7, p = 0.382).

VU0255035 inhibits pilocarpine-induced seizures and reduces pilocarpine-induced mortality in mice.

The data presented above provide strong evidence that VU0255035 is a highly selective orthosteric antagonist of M_1 and that this compound is effective as an M_1 antagonist in the hippocampal formation. To further evaluate the selectivity of this compound, we determined the activity of VU0255035 in binding to a large panel of GPCRs, ion channels, transporters and kinases using a MDS Pharma screen of the LeadProfilingScreen® series of potential targets (http://discovery.mdsps.com/Catalog/Discovery/AssayPackage.aspx?id=68). VU0255035 was devoid of significant activity at all targets included in this screen (**Suplemental Table 1**) when assayed at a concentration of 10 μM. Thus, VU0255035 is highly selective for M_1 relative to other mAChR subtypes or multiple other known targets and could provide an unprecedented opportunity to determine the effects of selective blockade of M_1 *in vivo*. To evaluate VU0255035 as a potential reagent for *in vivo* studies, we performed pharmacokinetics (PK) studies to determine whether VU0255035 achieves reasonable brain exposure when dosed systemically. After intraperitoneal (i.p.) administration, VU0255035 was rapidly absorbed into systemic circulation and into brain (**Supplemental Figure 2**). The maximum concentration in the brain and plasma (T_{max}) was achieved within 0.5 h. The Brain AUC(0-8)/Plasma AUC(0-8) ratio was

Downloaded from molpharm.aspetjournals.org at ASPET Journals on April 20, 2024

Molecular Pharmacology Fast Forward. Published on April 30, 2009 as DOI: 10.1124/mol.109.056531
This article has not been copyedited and formatted. The final version may differ from this version.

determined to be 0.48, indicating that VU0255035 shows excellent properties in terms of its ability to cross the blood brain barrier. The C_{max} of this compound was 1307.89 ± 327.69 ng/mL for plasma and 251.32 ± 168.32 ng/g for the brain. The elimination half-life ($T_{1/2}$) of VU0255035 was 1.29 h for the plasma and 2.58 h for the brain. While these PK studies do not provide information about oral bioavailability or other PK parameters after oral dosing, these data suggest that VU0255035 has PK properties that make it useful as a research tool for i.p. dosing.

Having established that VU0255035 achieves acceptable brain penetration following i.p. administration, we evaluated the effects of this compound in blocking pilocarpine-induced seizures *in vivo*. Pilocarpine, a mixed M_1/M_4 agonist, has been demonstrated to induce seizures via the M_1 mAChR subtype (Hamilton et al., 1997). To determine whether VU0255035 can inhibit pilocarpine-induced seizures in mice, C57Bk:129Sv mice, 2-6 months old, were dosed i.p. with methylscopolamine nitrate (1 mg/kg) to block the peripheral effects of pilocarpine, followed immediately by i.p. injections of either vehicle or VU0255035 (10 mg/kg). Finally, 30 minutes after the vehicle or VU0255035 injection, the mice were dosed with an i.p. injection of pilocarpine (280 mg/kg). Seizures were graded based on a modified Racine scale for the first 45 min after pilocarpine injection as outlined in the Materials and Methods. These time points were chosen based on pharmacokinetic analysis and corresponded to the maximal brain exposure of VU0255035. VU0255035 caused a statistically significant decrease in pilocarpine-induced seizure scores as analyzed by two-way ANOVA, $p < 0.0001$ for the time-course. In addition, post hoc analyses of each time point demonstrated significant differences at the 35 minute ($p < 0.05$) and 40 minute time point ($p < 0.01$) following pilocarpine injection (**Figure 10**). Furthermore, VU0255035 reduced pilocarpine-induced mortality at 24 h post pilocarpine treatment with 67.5% mortality in the vehicle treated controls versus 25% mortality in the

Downloaded from molpharm.aspetjournals.org at ASPET Journals on April 20, 2024

Molecular Pharmacology Fast Forward. Published on April 30, 2009 as DOI: 10.1124/mol.109.056531
This article has not been copyedited and formatted. The final version may differ from this version.

VU0255035 treated group. Together, these data demonstrate that VU0255035 antagonizes the M_1 mAChR *in vivo*.

VU0255035 does not disrupt the acquisition of contextual fear conditioning, a preclinical model of learning and memory.

A major potential concern with the use of M_1 antagonists as potential therapeutic agents is that these compounds may impair cognitive function. This is based on the severe cognition-impairing effects of non-selective mAChR antagonists and the possibility that blockade of M_1 could play a role in impairing cognitive function. Having demonstrated the efficacy of VU0255035 for reversal of pilocarpine-induced seizures, we next wanted to evaluate the dose-dependent effects of VU0255035 on the acquisition of contextual fear conditioning, a model of hippocampal-dependent learning and memory in which rats exhibit increased freezing behavior or passive fear response in the context or environment in which they previously experienced an adverse stimulus such as a mild footshock (Phillips and LeDoux, 1992). Previous studies have shown that the non-selective muscarinic antagonist scopolamine produces dose-dependent deficits in the acquisition of the contextual fear conditioning response (Anagnostaras et al., 1995). However, prior to the development of VU0255035, the role of M_1 muscarinic receptors in this form of hippocampal-dependent learning and memory remained unclear as M_1 mAChR knockout mice have been shown to exhibit either normal (Miyakawa et al., 2001) or enhanced (Anagnostaras et al., 2003) contextual fear acquisition, suggesting that M_1 mAChRs may not be required for memory formation or for initial stability of memory in hippocampus.

In this task, male Sprague-Dawley rats were habituated to handling and injections for two consecutive days prior to the training day. On training day, rats were pretreated with vehicle or

Downloaded from molpharm.aspetjournals.org at ASPET Journals on April 20, 2024

Molecular Pharmacology Fast Forward. Published on April 30, 2009 as DOI: 10.1124/mol.109.056531
This article has not been copyedited and formatted. The final version may differ from this version.

various doses of scopolamine (0.03 – 0.3 mg/kg, s.c.) 15 min, or VU0255035 (3 – 30 mg/kg, i.p.) 30 min, prior to testing. Rats were then placed in the fear conditioning test chamber. Following a two min habituation period, rats were exposed to four presentations of a conditioned stimulus (CS), which consisted of a tone (5000 Hz, 70 dB) lasting 30 s. During the last 1 s of this CS period, each rat was exposed to an unconditioned stimulus (US), a continuous foot shock (0.5 mA). Both the tone (CS) and shock (US) were co-terminated. Approximately 24 h later, rats were given a 7 min contextual conditioning test in the same chamber in which they were trained. Memory of the fear response at this 24 h time point was assessed by recording the amount of freezing response in the testing chamber environment. Freezing was defined as a motionless posture, except for respiratory movements. Within a dose range tested, VU0255035 had no effect on the acquisition of the contextual fear conditioning response (**Figure 11A**) consistent with the lack of deficits on contextual freezing behavior reported in the M_1 knockout mice (Anagnostaras et al., 2003; Miyakawa et al., 2001). In contrast, scopolamine produced dose-dependent deficits in contextual fear response as shown by a significant decrease in freezing behavior, consistent with published findings (Anagnostaras et al., 2003; Miyakawa et al., 2001) (**Figure 11B**).

Downloaded from molpharm.aspetjournals.org at ASPET Journals on April 20, 2024

Molecular Pharmacology Fast Forward. Published on April 30, 2009 as DOI: 10.1124/mol.109.056531
This article has not been copyedited and formatted. The final version may differ from this version.

Discussion

Cholinergic pathways provide neuromodulatory systems involved in regulating multiple aspects of brain function. Based on this broad influence of cholinergic systems in the CNS, it is surprising that there have not been greater advances in development of therapeutic agents that target cholinergic signaling. A major challenge with regulation of cholinergic signaling is that all cholinergic agents developed thus far have dose limiting adverse effects that prevent widespread use in the clinic (Brocks, 1999; Holden and Kelly, 2002; Langmead et al., 2008; Wess et al., 2007). Theoretically, agents that selectively activate or block individual subtypes of ACh receptors could provide beneficial effects of modulating specific aspects of cholinergic systems without inducing the broad range of peripheral and central adverse effects. For instance, multiple efforts have focused on discovery and development of highly selective agonists or allosteric activators of M_1 or M_4 for treatment of Alzheimer's disease or schizophrenia (see (Conn et al., 2009) for review).

While discovery of selective activators of mAChRs has been a major focus of previous efforts, multiple studies suggest that selective antagonists of individual mAChR subtypes may also have important utility for treatment of CNS disorders. For instance, non-selective mAChR antagonists such as trihexyphenidyl have clearly established efficacy in the treatment of certain movement disorders, such as PD and dystonia (Pisani et al., 2007). While the precise mechanism of action of mAChR antagonists in treatment of PD and dystonia are not known, it is likely that these drugs act by modulating activity in the basal ganglia motor circuit by actions in the striatum (Pisani et al., 2007). M_1 and M_4 mAChRs are the most likely candidates for mediating these motor effects of mAChR antagonists (Hersch et al., 1994; Potter et al., 2004; Potter and Purkerson, 1995; Santiago and Potter, 2001). In addition, selective antagonists of mAChR

Downloaded from molpharm.aspetjournals.org at ASPET Journals on April 20, 2024

Molecular Pharmacology Fast Forward. Published on April 30, 2009 as DOI: 10.1124/mol.109.056531
This article has not been copyedited and formatted. The final version may differ from this version.

subtypes have potential utility in treatment of obesity (Maresca and Supuran, 2008), drug dependence (Langmead et al., 2008), and certain epileptic disorders (Hamilton et al., 1997). Of these, selective M_1 antagonists represent an especially attractive target for treatment of movement disorders and some forms of epilepsy. Discovery and characterization of a highly selective M_1 antagonist represents a major breakthrough and provides the first selective small molecule antagonist for the M_1 mAChR subtype. Furthermore, optimization of our original HTS hit to yield VU0255035 as a systemically active M_1 mAChR antagonist allows use of this compound for *in vivo* studies of the behavioral effects of selective blockade this receptor subtype. Consistent with previous studies suggesting that M_1 is the major mAChR subtype involved in induction of seizures by excessive activation of cholinergic systems, VU0255035 reduced pilocarpine-induced seizures.

While M_1 mAChR antagonists have been postulated to have potential utility in treatment of CNS disorders, a major concern that has reduced focus on discovery and development of mAChR antagonists is the possibility that these agents could induce severe cognitive disturbances. Anticholinergics have long been associated with induction of transient cognitive deficits in humans (Drachman and Leavitt, 1974) and in animal models (Fornari et al., 2000; Hagan et al., 1987). Despite their efficacy in some CNS disorders, impairments in cognitive function, along with peripheral adverse effects, have prevented widespread clinical use of mAChR antagonists. While blockade of M_2 and M_3 mAChRs are thought be responsible for most peripheral adverse effects (Wess et al., 2007), blockade of M_1 may play a major role in impaired cognitive function. M_1 is highly expressed in the hippocampus and other forebrain regions (Levey et al., 1991) where mAChRs play critical roles in regulation of neuronal excitability and synaptic transmission (Shirey et al., 2008; Wess et al., 2007). Based on early findings that M_1 is

Downloaded from molpharm.aspetjournals.org at ASPET Journals on April 20, 2024

Molecular Pharmacology Fast Forward. Published on April 30, 2009 as DOI: 10.1124/mol.109.056531
This article has not been copyedited and formatted. The final version may differ from this version.

heavily expressed in these regions, this receptor was postulated to play a critical role in learning and memory. However, more recent studies reveal that mAChR regulation of excitability of hippocampal pyramidal cells is not altered in M_1 mAChR knockout mice (Rouse et al., 2000), suggesting that M_1 is not the major mAChR subtype responsible for regulating excitability of these cells. Furthermore, while M_1 is the primary mAChR subtype involved in modulation of NMDA receptor currents in these cells (Jones et al., 2008; Marino et al., 1998), this receptor is not responsible for acute modulation of transmission at excitatory or inhibitory synapses in the hippocampus (Jones et al., 2008; Rouse et al., 1999; Shirey et al., 2008). Thus, it is likely that multiple mAChR subtypes are critical for regulating hippocampal and cortical function and that M_1 does not play as dominant a role as was once assumed. Consistent with this, studies in M_1 mAChR knockout mice revealed that performance in hippocampal-dependent learning tasks including Morris water maze and contextual fear acquisition remain intact or may be enhanced after deletion of the M_1 gene (Anagnostaras et al., 2003; Miyakawa et al., 2001). Furthermore, Anagnostras et al. (2003) found that scopolamine induced comparable impairments in the Morris water maze paradigm in M_1 mAChR knockout and WT mice, indicating that other non-M_1 mAChRs clearly must play a critical role in hippocampal-dependent learning and memory (Anagnostaras et al., 2003). Our present finding that VU0255035 does not induce deficits in contextual fear acquisition is consistent with the M_1 mAChR knockout mouse data and provides initial evidence that selective M_1 antagonists may not induce the same severity of cognitive deficits associated with the non-selective anticholinergics. In future studies, it will be important to determine the effects of VU0255035 in a range of models of other forms of cognitive function to gain a more complete understanding of the roles of M_1 in different forms of learning and memory and further assess the potential adverse effect liability of M_1-selective antagonists. In

Downloaded from molpharm.aspetjournals.org at ASPET Journals on April 20, 2024

Molecular Pharmacology Fast Forward. Published on April 30, 2009 as DOI: 10.1124/mol.109.056531
This article has not been copyedited and formatted. The final version may differ from this version.

addition, VU0255035 provides a valuable tool to allow further studies of the physiological roles of M_1 in the hippocampus, cortex, and other brain regions heavily modulated by cholinergic afferents.

It was somewhat surprising that we were able to achieve the high M_1-subtype selectivity observed with VU0255035 with a compound that targets the orthosteric (ACh) binding site. The orthosteric site of the mAChRs is highly conserved (Felder et al., 2000) and previous efforts to develop this level of M_1-subtype selectivity with orthosteric ligands have been largely unsuccessful. In contrast, recent efforts to develop ligands for less conserved allosteric sites on mAChRs have yielded highly selective positive allosteric modulators (PAMs) of individual mAChR subtypes (see (Conn et al., 2009) for review). Given the functional selectivity of VU0255035 for M_1 relative to M_2-M_5 mAChR subtypes, we initially expected that VU0255035 was likely acting as an allosteric antagonist of M_1 mAChRs. However, multiple studies, including Scatchard analysis, Schild analysis, and mutagenesis studies, provide strong evidence that VU0255035 is a competitive orthosteric M_1 antagonist. These data do not rule out the possibility that VU0255035 binds to a site that partially overlaps with the orthosteric binding site. Additional mutagenesis studies and binding studies will be necessary to fully evaluate the binding pocket for VU0255035.

In summary, VU0255035 is a highly selective orthosteric antagonist of M_1 mAChRs. This compound demonstrates selective M_1 mAChR antagonism both *in vitro* and *in vivo* as demonstrated through *in vitro* functional studies, the inhibition of PI hydrolysis induced by CCh in hippocampal slices, and the inhibition CCh-induced NMDA receptor potentiation in the hippocampus. VU0255035's *in vivo* efficacy for the inhibition of pilocarpine-induced seizures, lack of effect on hippocampal-dependent contextual fear acquisition, combined with

Downloaded from molpharm.aspetjournals.org at ASPET Journals on April 20, 2024

Molecular Pharmacology Fast Forward. Published on April 30, 2009 as DOI: 10.1124/mol.109.056531
This article has not been copyedited and formatted. The final version may differ from this version.

pharmacokinetic data indicates that VU0255035 is rapidly taken up into the brain provide valuable data demonstrating VU0255035's utility as a novel tool that can be utilized to evaluate the role of M_1 mAChRs antagonists as a novel approach for the treatment of PD, dystonia, and other movement disorders and that the use of selective M_1 mAChR antagonists as therapeutics may not induce severe cognitive deficits. VU0255035 is a MLCSN probe available for free upon request by the identifier, CID24768606.

Downloaded from molpharm.aspetjournals.org at ASPET Journals on April 20, 2024

Molecular Pharmacology Fast Forward. Published on April 30, 2009 as DOI: 10.1124/mol.109.056531
This article has not been copyedited and formatted. The final version may differ from this version.

References

Anagnostaras SG, Maren S and Fanselow MS (1995) Scopolamine selectively disrupts the acquisition of contextual fear conditioning in rats. *Neurobiol Learn Mem* **64**(3):191-194.

Anagnostaras SG, Murphy GG, Hamilton SE, Mitchell SL, Rahnama NP, Nathanson NM and Silva AJ (2003) Selective cognitive dysfunction in acetylcholine M1 muscarinic receptor mutant mice. *Nat Neurosci* **6**(1):51-58.

Arunlakshana O and Schild HO (1959) Some quantitative uses of drug antagonists. *Br J Pharmacol Chemother* **14**(1):48-58.

Brocks DR (1999) Anticholinergic drugs used in Parkinson's disease: An overlooked class of drugs from a pharmacokinetic perspective. *J Pharm Pharm Sci* **2**(2):39-46.

Bymaster FP, Carter PA, Yamada M, Gomeza J, Wess J, Hamilton SE, Nathanson NM, McKinzie DL and Felder CC (2003a) Role of specific muscarinic receptor subtypes in cholinergic parasympathomimetic responses, in vivo phosphoinositide hydrolysis, and pilocarpine-induced seizure activity. *Eur J Neurosci* **17**(7):1403-1410.

Bymaster FP and Falcone JF (2000) Decreased binding affinity of olanzapine and clozapine for human muscarinic receptors in intact clonal cells in physiological medium. *Eur J Pharmacol* **390**(3):245-248.

Bymaster FP, Felder CC, Tzavara E, Nomikos GG, Calligaro DO and McKinzie DL (2003b) Muscarinic mechanisms of antipsychotic atypicality. *Prog Neuropsychopharmacol Biol Psychiatry* **27**(7):1125-1143.

Downloaded from molpharm.aspetjournals.org at ASPET Journals on April 20, 2024

Molecular Pharmacology Fast Forward. Published on April 30, 2009 as DOI: 10.1124/mol.109.056531
This article has not been copyedited and formatted. The final version may differ from this version.

Conn PJ, Jones CK and Lindsley CW (2009) Subtype-selective allosteric modulators of muscarinic receptors for the treatment of CNS disorders. *Trends Pharmacol Sci* **30**(3):148-155.

Conn PJ and Sanders-Bush E (1986) Biochemical characterization of serotonin stimulated phosphoinositide turnover. *Life Sci* **38**(7):663-669.

Drachman DA and Leavitt J (1974) Human memory and the cholinergic system. A relationship to aging? *Arch Neurol* **30**(2):113-121.

Felder CC, Bymaster FP, Ward J and DeLapp N (2000) Therapeutic opportunities for muscarinic receptors in the central nervous system. *J Med Chem* **43**(23):4333-4353.

Fornari RV, Moreira KM and Oliveira MG (2000) Effects of the selective M1 muscarinic receptor antagonist dicyclomine on emotional memory. *Learn Mem* **7**(5):287-292.

Hagan JJ, Jansen JH and Broekkamp CL (1987) Blockade of spatial learning by the M1 muscarinic antagonist pirenzepine. *Psychopharmacology (Berl)* **93**(4):470-476.

Hamilton SE, Loose MD, Qi M, Levey AI, Hille B, McKnight GS, Idzerda RL and Nathanson NM (1997) Disruption of the m1 receptor gene ablates muscarinic receptor-dependent M current regulation and seizure activity in mice. *Proc Natl Acad Sci U S A* **94**(24):13311-13316.

Hersch SM, Gutekunst CA, Rees HD, Heilman CJ and Levey AI (1994) Distribution of m1-m4 muscarinic receptor proteins in the rat striatum: light and electron microscopic immunocytochemistry using subtype-specific antibodies. *J Neurosci* **14**(5 Pt 2):3351-3363.

Holden M and Kelly C (2002) Use of cholinesterase inhibitors in dementia. *Advances in Psychiatric Treatment* **8**:89-96.

Downloaded from molpharm.aspetjournals.org at ASPET Journals on April 20, 2024

Molecular Pharmacology Fast Forward. Published on April 30, 2009 as DOI: 10.1124/mol.109.056531
This article has not been copyedited and formatted. The final version may differ from this version.

Jones CK, Brady AE, Davis AA, Xiang Z, Bubser M, Tantawy MN, Kane AS, Bridges TM, Kennedy JP, Bradley SR, Peterson TE, Ansari MS, Baldwin RM, Kessler RM, Deutch AY, Lah JJ, Levey AI, Lindsley CW and Conn PJ (2008) Novel selective allosteric activator of the M1 muscarinic acetylcholine receptor regulates amyloid processing and produces antipsychotic-like activity in rats. *J Neurosci* **28**(41):10422-10433.

Karlsson E, Jolkkonen M, Mulugeta E, Onali P and Adem A (2000) Snake toxins with high selectivity for subtypes of muscarinic acetylcholine receptors. *Biochimie* **82**(9-10):793-806.

Kennedy JP, Williams L, Bridges TM, Daniels RN, Weaver D and Lindsley CW (2008) Application of combinatorial chemistry science on modern drug discovery. *J Comb Chem* **10**(3):345-354.

Langmead CJ, Watson J and Reavill C (2008) Muscarinic acetylcholine receptors as CNS drug targets. *Pharmacol Ther* **117**(2):232-243.

Leister W, Strauss K, Wisnoski D, Zhao Z and Lindsley C (2003) Development of a custom high-throughput preparative liquid chromatography/mass spectrometer platform for the preparative purification and analytical analysis of compound libraries. *J Comb Chem* **5**(3):322-329.

Levey AI, Kitt CA, Simonds WF, Price DL and Brann MR (1991) Identification and localization of muscarinic acetylcholine receptor proteins in brain with subtype-specific antibodies. *J Neurosci* **11**(10):3218-3226.

Lewis LM, Sheffler D, Williams R, Bridges TM, Kennedy JP, Brogan JT, Mulder MJ, Williams L, Nalywajko NT, Niswender CM, Weaver CD, Conn PJ and Lindsley CW (2008)

Downloaded from molpharm.aspetjournals.org at ASPET Journals on April 20, 2024

Molecular Pharmacology Fast Forward. Published on April 30, 2009 as DOI: 10.1124/mol.109.056531
This article has not been copyedited and formatted. The final version may differ from this version.

Synthesis and SAR of selective muscarinic acetylcholine receptor subtype 1 (M1 mAChR) antagonists. *Bioorg Med Chem Lett* **18**(3):885-890.

Maresca A and Supuran CT (2008) Muscarinic acetylcholine receptors as therapeutic targets for obesity. *Expert Opin Ther Targets* **12**(9):1167-1175.

Marino MJ, Rouse ST, Levey AI, Potter LT and Conn PJ (1998) Activation of the genetically defined m1 muscarinic receptor potentiates N-methyl-D-aspartate (NMDA) receptor currents in hippocampal pyramidal cells. *Proc Natl Acad Sci U S A* **95**(19):11465-11470.

Messer WS, Jr. (2002) The utility of muscarinic agonists in the treatment of Alzheimer's disease. *J Mol Neurosci* **19**(1-2):187-193.

Miyakawa T, Yamada M, Duttaroy A and Wess J (2001) Hyperactivity and intact hippocampus-dependent learning in mice lacking the M1 muscarinic acetylcholine receptor. *J Neurosci* **21**(14):5239-5250.

Phillips RG and LeDoux JE (1992) Differential contribution of amygdala and hippocampus to cued and contextual fear conditioning. *Behav Neurosci* **106**(2):274-285.

Pisani A, Bernardi G, Ding J and Surmeier DJ (2007) Re-emergence of striatal cholinergic interneurons in movement disorders. *Trends Neurosci* **30**(10):545-553.

Porter AC, Bymaster FP, DeLapp NW, Yamada M, Wess J, Hamilton SE, Nathanson NM and Felder CC (2002) M1 muscarinic receptor signaling in mouse hippocampus and cortex. *Brain Res* **944**(1-2):82-89.

Potter LT, Flynn DD, Liang JS and McCollum MH (2004) Studies of muscarinic neurotransmission with antimuscarinic toxins. *Prog Brain Res* **145**:121-128.

Downloaded from molpharm.aspetjournals.org at ASPET Journals on April 20, 2024

Molecular Pharmacology Fast Forward. Published on April 30, 2009 as DOI: 10.1124/mol.109.056531
This article has not been copyedited and formatted. The final version may differ from this version.

Potter LT and Purkerson SL (1995) Pharmacology of striatal muscarinic receptors, in *Molecular and Cellular Mechanisms of Neostriatal Function* (Ariano M, Surmeier, J. ed) pp 241-254, R.G. Landes Co., New York.

Rouse ST, Hamilton SE, Potter LT, Nathanson NM and Conn PJ (2000) Muscarinic-induced modulation of potassium conductances is unchanged in mouse hippocampal pyramidal cells that lack functional M1 receptors. *Neurosci Lett* **278**(1-2):61-64.

Rouse ST, Marino MJ, Potter LT, Conn PJ and Levey AI (1999) Muscarinic receptor subtypes involved in hippocampal circuits. *Life Sci* **64**(6-7):501-509.

Santiago MP and Potter LT (2001) Biotinylated m4-toxin demonstrates more M4 muscarinic receptor protein on direct than indirect striatal projection neurons. *Brain Res* **894**(1):12-20.

Shirey JK, Xiang Z, Orton D, Brady AE, Johnson KA, Williams R, Ayala JE, Rodriguez AL, Wess J, Weaver D, Niswender CM and Conn PJ (2008) An allosteric potentiator of M4 mAChR modulates hippocampal synaptic transmission. *Nat Chem Biol* **4**(1):42-50.

Spalding TA, Ma JN, Ott TR, Friberg M, Bajpai A, Bradley SR, Davis RE, Brann MR and Burstein ES (2006) Structural requirements of transmembrane domain 3 for activation by the M1 muscarinic receptor agonists AC-42, AC-260584, clozapine, and N-desmethylclozapine: evidence for three distinct modes of receptor activation. *Mol Pharmacol* **70**(6):1974-1983.

Sur C, Mallorga PJ, Wittmann M, Jacobson MA, Pascarella D, Williams JB, Brandish PE, Pettibone DJ, Scolnick EM and Conn PJ (2003) N-desmethylclozapine, an allosteric agonist at muscarinic 1 receptor, potentiates N-methyl-D-aspartate receptor activity. *Proc Natl Acad Sci U S A* **100**(23):13674-13679.

Downloaded from molpharm.aspetjournals.org at ASPET Journals on April 20, 2024

Molecular Pharmacology Fast Forward. Published on April 30, 2009 as DOI: 10.1124/mol.109.056531
This article has not been copyedited and formatted. The final version may differ from this version.

Wess J (2004) Muscarinic acetylcholine receptor knockout mice: novel phenotypes and clinical implications. *Annu Rev Pharmacol Toxicol* **44**:423-450.

Wess J, Eglen RM and Gautam D (2007) Muscarinic acetylcholine receptors: mutant mice provide new insights for drug development. *Nat Rev Drug Discov* **6**(9):721-733.

Downloaded from molpharm.aspetjournals.org at ASPET Journals on April 20, 2024

Molecular Pharmacology Fast Forward. Published on April 30, 2009 as DOI: 10.1124/mol.109.056531
This article has not been copyedited and formatted. The final version may differ from this version.

Footnotes

This work was supported by the National Institutes of Health grants [3U54MH074427, 3U54MH074427-02S1, and 1XO1MH077606-01] (to C.D.W.), [1U54MH084659] (to C.W.L.); the Dystonia Medical Research Foundation (to Z.X.); and a PhRMA Foundation Award (to D.J.S.).

Downloaded from molpharm.aspetjournals.org at ASPET Journals on April 20, 2024

Molecular Pharmacology Fast Forward. Published on April 30, 2009 as DOI: 10.1124/mol.109.056531
This article has not been copyedited and formatted. The final version may differ from this version.

Figure Legends

Figure 1. HTS lead 1 displays M_1 versus M_4 mAChR selective antagonism. Inset is the structure of compound 1. CRCs of compound 1 were performed in the presence of an EC_{80} concentration of ACh for each receptor in a calcium mobilization assay. Data were normalized to the maximum response to 10 μM ACh and are presented as the % of the EC_{80} ACh response. The IC_{50} for compound 1 inhibition of an EC_{80} ACh response is 2.4 ± 1.2 uM for M_1. The M_4 mAChR calculated IC_{50} is greater than 150 μM. All data points represent the mean of three independent experiments performed in triplicate and error bars represent S.E.M.

Figure 2. Chemical optimization generates compounds that antagonize M_1 mAChRs with greater potency than HTS lead 1. (A) Functionalized piperazine amides represented by structure **5.** (B) CRCs of compounds were performed in the presence of an EC_{80} concentration of ACh for M_1 mAChRs in a calcium mobilization assay. Data were normalized to the maximum response to 10 μM ACh and are presented as the % of the EC_{80} ACh response. The IC_{50} for 5a inhibition of an EC_{80} ACh response is 3.2 ± 1.6 μM. The IC_{50} for 5b inhibition of an EC_{80} ACh response is 309.1 ± 100.5 nM. All other calculated IC_{50}s are greater than 10 μM. All data points represent the mean of three independent experiments performed in triplicate and error bars represent S.E.M.

Figure 3. VU0255035 selectively antagonizes the M_1 mAChR relative to other mAChRs. CRCs of VU0255035 were performed in the presence of an EC_{80} concentration of ACh for each receptor in a calcium mobilization assay. Data were normalized to the maximum response to 10

Downloaded from molpharm.aspetjournals.org at ASPET Journals on April 20, 2024

Molecular Pharmacology Fast Forward. Published on April 30, 2009 as DOI: 10.1124/mol.109.056531
This article has not been copyedited and formatted. The final version may differ from this version.

μM ACh and are presented as the % of the EC_{80} ACh response. The IC_{50} for VU0255035 inhibition of an EC_{80} ACh response is 132.6 ± 28.5 nM for M_1. All other calculated IC_{50}s are greater than 5 μM. All data points represent the mean of five independent experiments performed in triplicate and error bars represent S.E.M.

Figure 4. VU0255035 competes [^{3}H]-NMS binding at M_1-M_5 mAChRs and displays M_1 selectivity. (A) Binding of 0.1 nM [^{3}H]-NMS was displaced by VU0255035 at M_1-M_5 mAChRs. (B) Binding of 0.1 nM [^{3}H]-NMS was displaced by atropine at M_1-M_5 mAChRs. For all experiments, specific binding represented less than 10% of the total radioligand binding. All data points represent the mean of three independent experiments performed in triplicate and error bars represent S.E.M.

Figure 5. VU0255035 reduces [^{3}H]-NMS binding to M_1 mAChRs in a competitive manner. Scatchard analysis demonstrates that VU0255035 dose-dependently decreases [^{3}H]-NMS binding affinity but does not alter the B_{max}. Saturation binding experiments were performed on membranes from M_1 expressing CHO cells in the absence or presence of 10 nM, 30 nM, or 100 nM VU0255035. In the absence of VU0255035, the B_{max} was 562 ± 51 fmol/mg protein. With 10 nM, 30 nM, and 100 nM VU0255035 treated samples, the B_{max} was 554 ± 67, 583 ± 60, or 538 ± 54 fmol/mg protein respectively. There was no significant difference between the B_{max} values of [^{3}H]-NMS binding for the vehicle treated or any of the VU0255035 treated samples (Student's t test). Linear regression lines were generated from three independent experiments performed in duplicate. Error bars represent S.E.M.

Downloaded from molpharm.aspetjournals.org at ASPET Journals on April 20, 2024

Molecular Pharmacology Fast Forward. Published on April 30, 2009 as DOI: 10.1124/mol.109.056531
This article has not been copyedited and formatted. The final version may differ from this version.

Figure 6. VU0255035 competitively antagonizes the M_1 mAChR functional response to ACh but does not competitively antagonize the M_1 mAChR response to TBPB. (A) ACh CRCs in the absence or presence of 100 nM, 300 nM, 1 μM, or 3 μM VU0255035 in a calcium mobilization assay. (B) Schild regression of the dose ratios derived from the VU0255035 antagonism of ACh. The slope of this regression is 0.95 ± 0.16 with a calculated K_d of 33 nM. (C) TBPB CRCs in the absence or presence of 100 nM, 1 μM, or 10 μM VU0255035 in a calcium mobilization assay. (D) Schild regression of the dose ratios derived from the VU0255035 antagonism of TBPB. The slope of this regression is 0.69 ± 0.06. Values represent the mean ± S.E.M. of 4 to 6 experiments conducted in triplicate.

Figure 7. The VU0255035 antagonism of M_1 mAChR responses are right shifted by Y381A mutation. (A) CRCs of ACh and NDMC were performed on both wild type (WT) and Y381A mutated M_1 mAChRs in a calcium mobilization assay. Data were normalized to either the maximum response to 1 μM ACh (WT) or to 10 mM ACh (Y381A) and are presented as the % maximal ACh response. The EC_{50}s for ACh were 2.5 ± 0.3 nM (WT) or 13.7 ± 1.6 μM (Y381A). The EC_{50}s for NDMC were 140.5 ± 26.1 nM (WT) or 162.4 ± 6.1 nM (Y381A). (B) CRCs of VU0255035 were performed in the presence of an EC_{80} concentration of ACh or NDMC for WT and Y381A M_1 mAChRs in a calcium mobilization assay. Data were normalized to the % of either the EC_{80} ACh response or the EC_{80} NDMC response. The IC_{50}s for VU0255035 versus ACh were 53.3 ± 7.7 nM (WT) or 38.9 ± 0.2 μM (Y381A). The IC_{50}s for VU0255035 versus NDMC were 57.3 ± 3.5 nM (WT) or 33.4 ± 8.4 μM (Y381A). All data points represent the mean of three independent experiments performed in triplicate and error bars represent S.E.M.

Downloaded from molpharm.aspetjournals.org at ASPET Journals on April 20, 2024

Molecular Pharmacology Fast Forward. Published on April 30, 2009 as DOI: 10.1124/mol.109.056531
This article has not been copyedited and formatted. The final version may differ from this version.

Figure 8. VU0255035 antagonizes PI hydrolysis in rat hippocampal slices induced by the mAChR agonist CCh. CRCs of VU0255035 were performed in the presence of an EC_{80} concentration of CCh for induction of PI hydrolysis in rat hippocampal slices. Data were normalized to the maximum response to 100 μM CCh and are presented as the % of the EC_{80} CCh response. The IC_{50} for VU0255035 inhibition of an EC_{80} CCh response is 2.4 ± 1.0 μM. All data points represent the mean of six independent experiments performed in triplicate and error bars represent S.E.M.

Figure 9. VU0255035 blocks the CCh-induced potentiation of NMDAR currents in CA1 pyramidal cells. (A) Representative traces of NMDA-evoked currents obtained from a typical experiment (*top*) and time course of normalized amplitude of NMDAR currents before, during and after application of 10 μM CCh (n = 9) (*bottom*). (B) Representative traces of NMDAR currents (*top*) and time course of normalized amplitude of NMDAR currents in control, during application of VU0255035 (5 μM) and application of VU0255035 with 10 μM CCh, and washout (n = 7) (*bottom*), showing the ability of VU0255035 to block CCh-induced potentiation of NMDAR currents. (C) Summary of the peak potentiation of NMDAR currents by 10 μM CCh in control (n = 9) and in the presence of VU0255035 (n = 7) (p = 0.016). Data represent mean ± S.E.M.

Figure 10. VU0255035 blocks pilocarpine-induced seizures in mice. For these studies, C57Bk:129Sv mice, 2-6 months old, were dosed i.p. with methylscopolamine nitrate (1 mg/kg) to block the peripheral effects of pilocarpine, followed immediately thereafter with i.p. injections of either vehicle or VU0255035 (10 mg/kg). Finally, 30 min after the vehicle or VU0255035

Downloaded from molpharm.aspetjournals.org at ASPET Journals on April 20, 2024

Molecular Pharmacology Fast Forward. Published on April 30, 2009 as DOI: 10.1124/mol.109.056531
This article has not been copyedited and formatted. The final version may differ from this version.

injection, the mice were dosed with an i.p. injection of pilocarpine (280 mg/kg). Seizures were graded based on a modified Racine scale as outlined in the Materials and Methods for the first 45 min after pilocarpine injection. The seizure scores for the first 45 min after pilocarpine injection for the control group and VU0255035 treated group were analyzed using 2-way ANOVA. VU0255035 caused a statistically significant decrease in pilocarpine-induced seizure scores as analyzed by two-way ANOVA, $p < 0.0001$. Post hoc analyses of individual timepoints demonstrated a significant difference at the 35 min (*, $p < 0.05$) and 40 min (**, $p < 0.01$) timepoints. All data points represent the mean of eight mice for the control group and six mice for the VU0255035 group.

Figure 11. VU0255035 does not affect acquisition of a contextual fear conditioning response whereas scopolamine induces deficits. (A) VU0255035 (3.0 – 10.0 mg/kg, i.p.) had no effect on the acquisition of contextual fear. (B) Scopolamine (0.03-0.3 mg/kg, s.c.) produced a robust dose-dependent disruption in the acquisition of contextual fear conditioning response as shown by a decrease in the percent of time spent freezing in the same context environment as the training session, significant after doses of 0.1, 0.2 and 0.3 mg/kg by a Dunnett's comparison with vehicle. Results are expressed as mean percent freezing behavior ± S.E.M. (n = 6-10 rats per treatment group). *$p < 0.05$ when compared with the vehicle control group.

Downloaded from molpharm.aspetjournals.org at ASPET Journals on April 20, 2024

Molecular Pharmacology Fast Forward. Published on April 30, 2009 as DOI: 10.1124/mol.109.056531
This article has not been copyedited and formatted. The final version may differ from this version.

Table 1. Apparent affinity values for VU0255035 and atropine for the competition of [^{3}H]-NMS binding from M_1-M_5 mAChRs.

	VU0255035 Ki (nM)	Fold Selectivity (VS M_1)	Atropine K_i (nM)
M_1	14.87 ± 0.66		0.80 ± 0.07
M_2	661.33 ± 57.64	45	2.60 ± 0.18
M_3	876.93 ± 151.44	59	1.09 ± 0.02
M_4	1177.67 ± 124.42	79	0.55 ± 0.31
M_5	2362.33 ± 577.49	159	1.64 ± 0.17

Ki values for VU0255035 and atropine were determined based on competition binding experiments with 0.1 nM [^{3}H]-NMS at each mAChR. The data represent the mean of three independent experiments performed in triplicate and error bars represent S.E.M.

Downloaded from molpharm.aspetjournals.org at ASPET Journals on April 20, 2024

Figure 1.

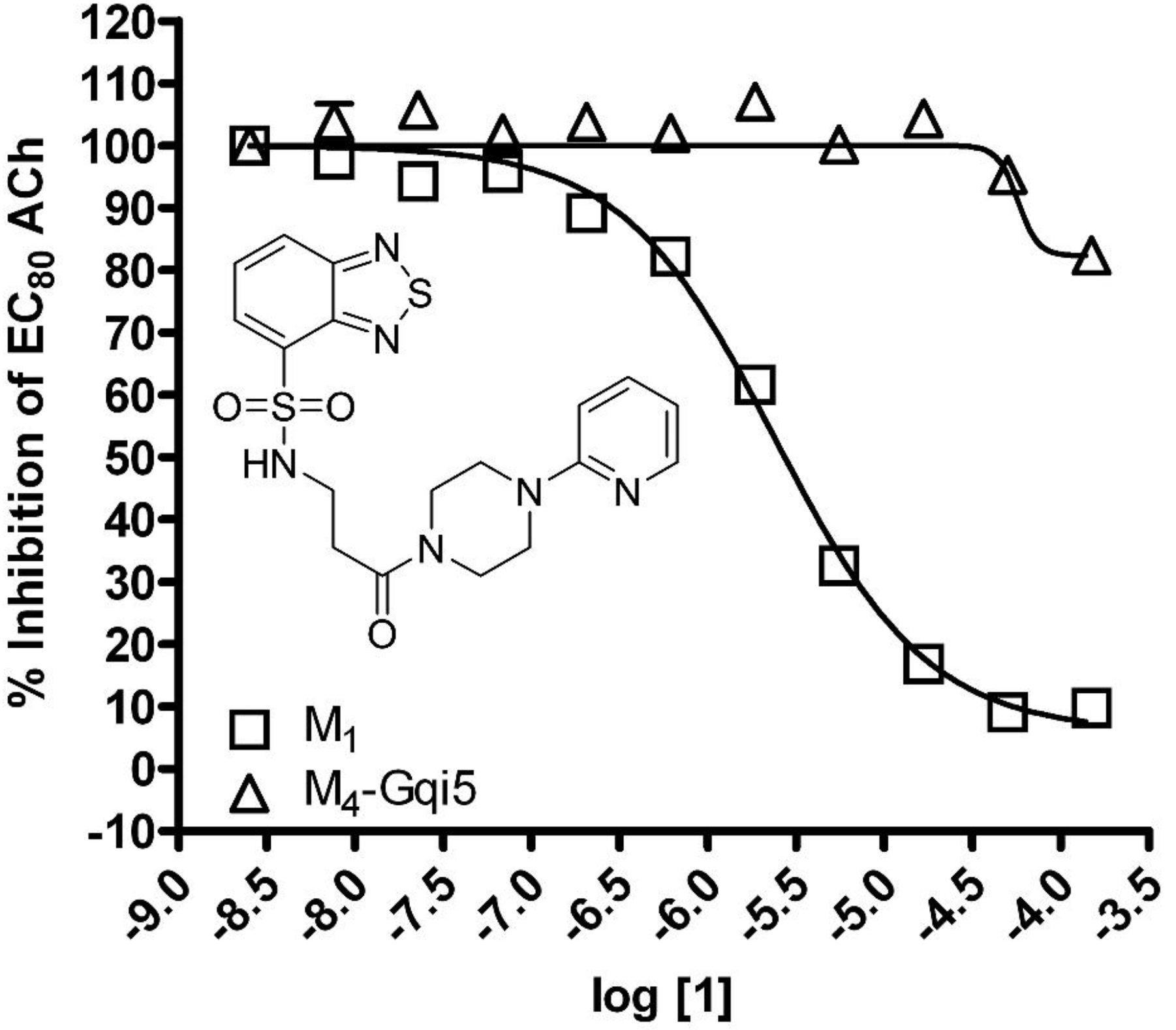
% Inhibition of EC_{80} ACh
120
110
100
90
80
70
60
50
40
30
20
10
0
-10
-9.0
-8.5
-8.0
-7.5
-7.0
-6.5
-6.0
-5.5
-5.0
-4.5
-4.0
-3.5
log [1]
M_1
M_4-Gqi5
N
S
N
O=S=O
HN
N
N
N
O

Figure 2.

A

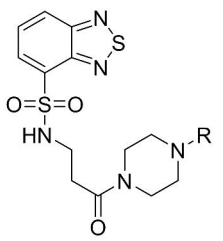

5a, 3-pyridyl

5b, 4-pyridyl

5c, Ph

5d, 2-pyrimidinyl

5e, 3-OMePh

5f, 2-CNPh

5g, 2-FPh

5h, *i*-Pr

B

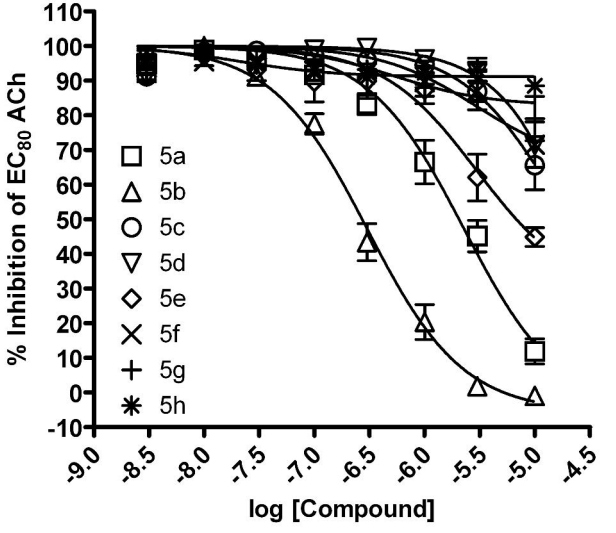

Figure 3.

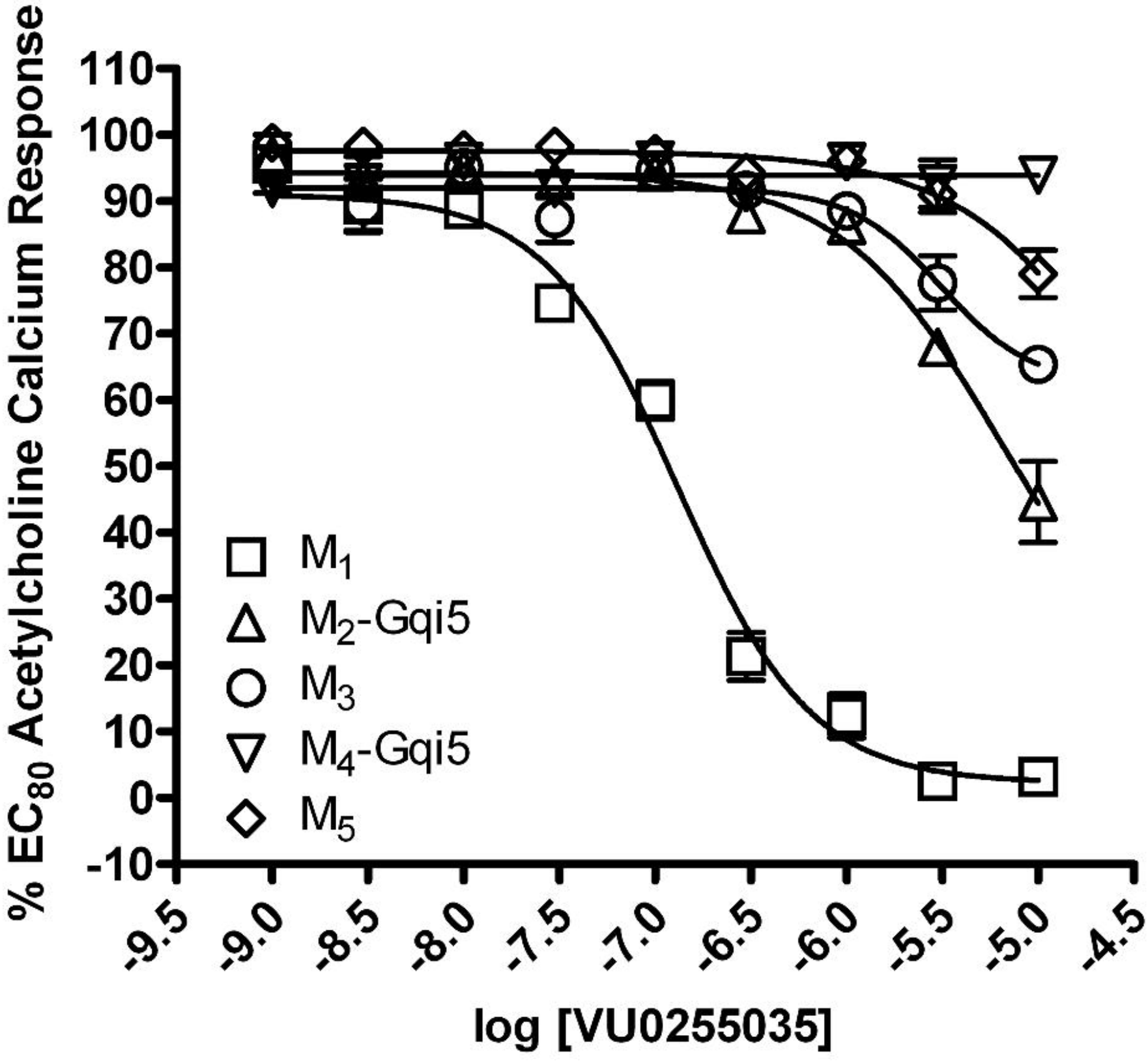
% EC80 Acetylcholine Calcium Response
110
100
90
80
70
60
50
40
30
20
10
0
-10
-9.5
-9.0
-8.5
-8.0
-7.5
-7.0
-6.5
-6.0
-5.5
-5.0
-4.5
log [VU0255035]
M1
M2-Gqi5
M3
M4-Gqi5
M5

Figure 4.

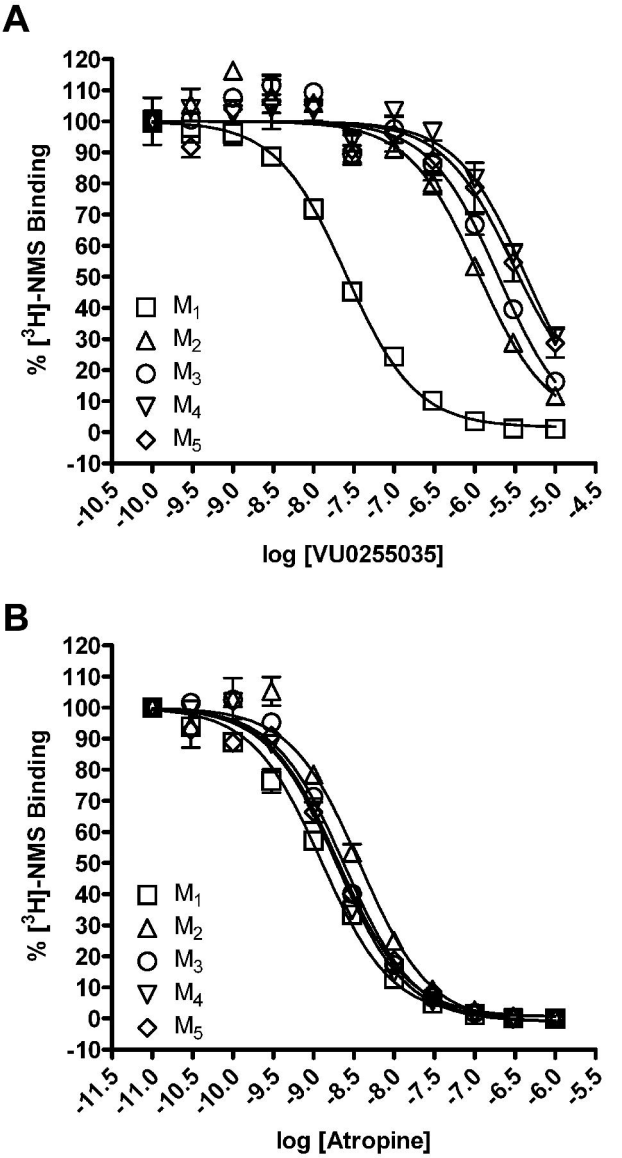
A
% [3H]-NMS Binding
120
110
100
90
80
70
60
50
40
30
20
10
0
-10
M1
M2
M3
M4
M5
-10.5
-10.0
-9.5
-9.0
-8.5
-8.0
-7.5
-7.0
-6.5
-6.0
-5.5
-5.0
-4.5
log [VU0255035]
B
% [3H]-NMS Binding
M1
M2
M3
M4
M5
-11.5
-11.0
-10.5
-10.0
-9.5
-9.0
-8.5
-8.0
-7.5
-7.0
-6.5
-6.0
-5.5
log [Atropine]

Figure 5.

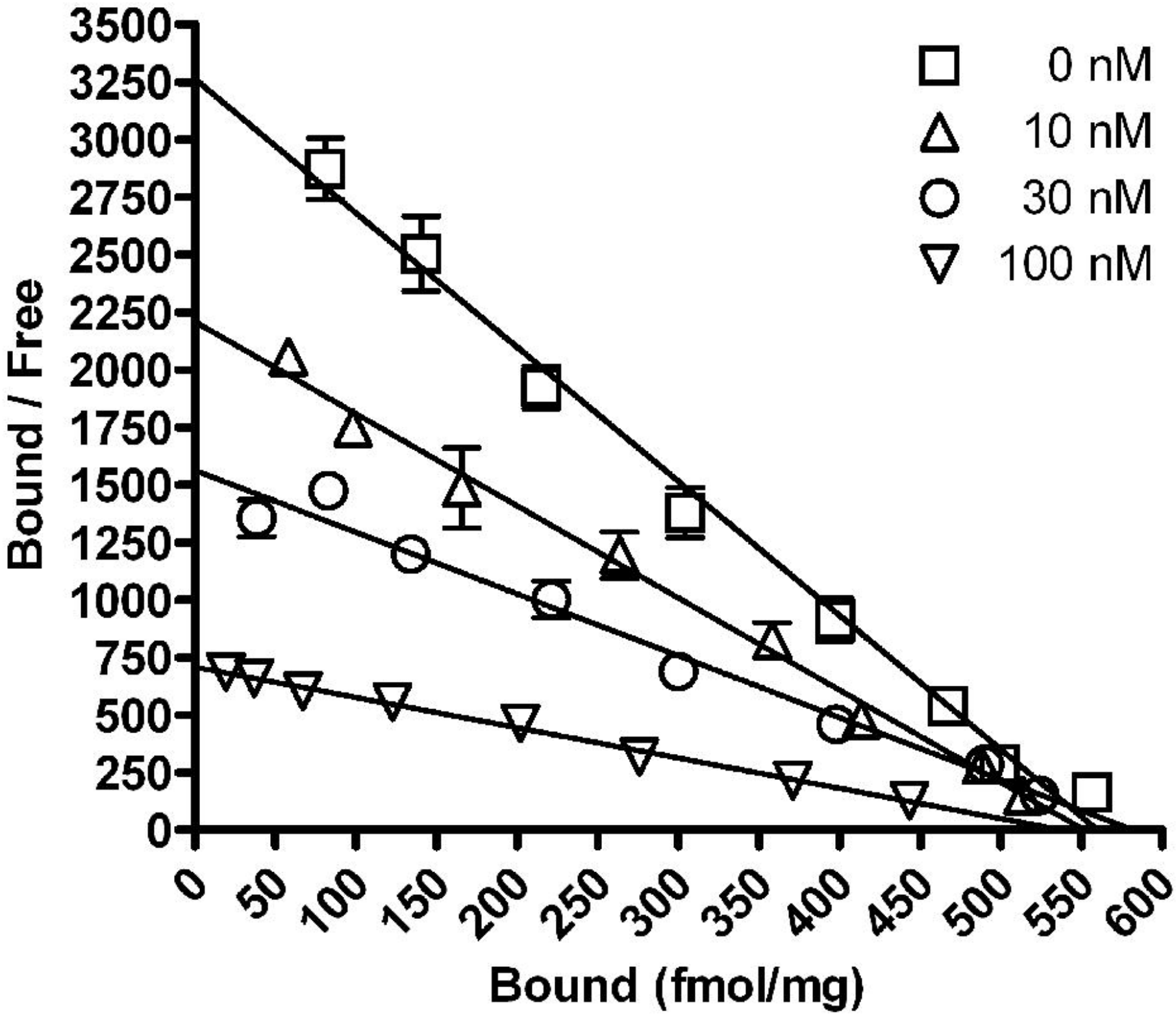
3500
3250
3000
2750
2500
2250
2000
1750
1500
1250
1000
750
500
250
0
Bound / Free
0
50
100
150
200
250
300
350
400
450
500
550
600
Bound (fmol/mg)
0 nM
10 nM
30 nM
100 nM

Figure 6.

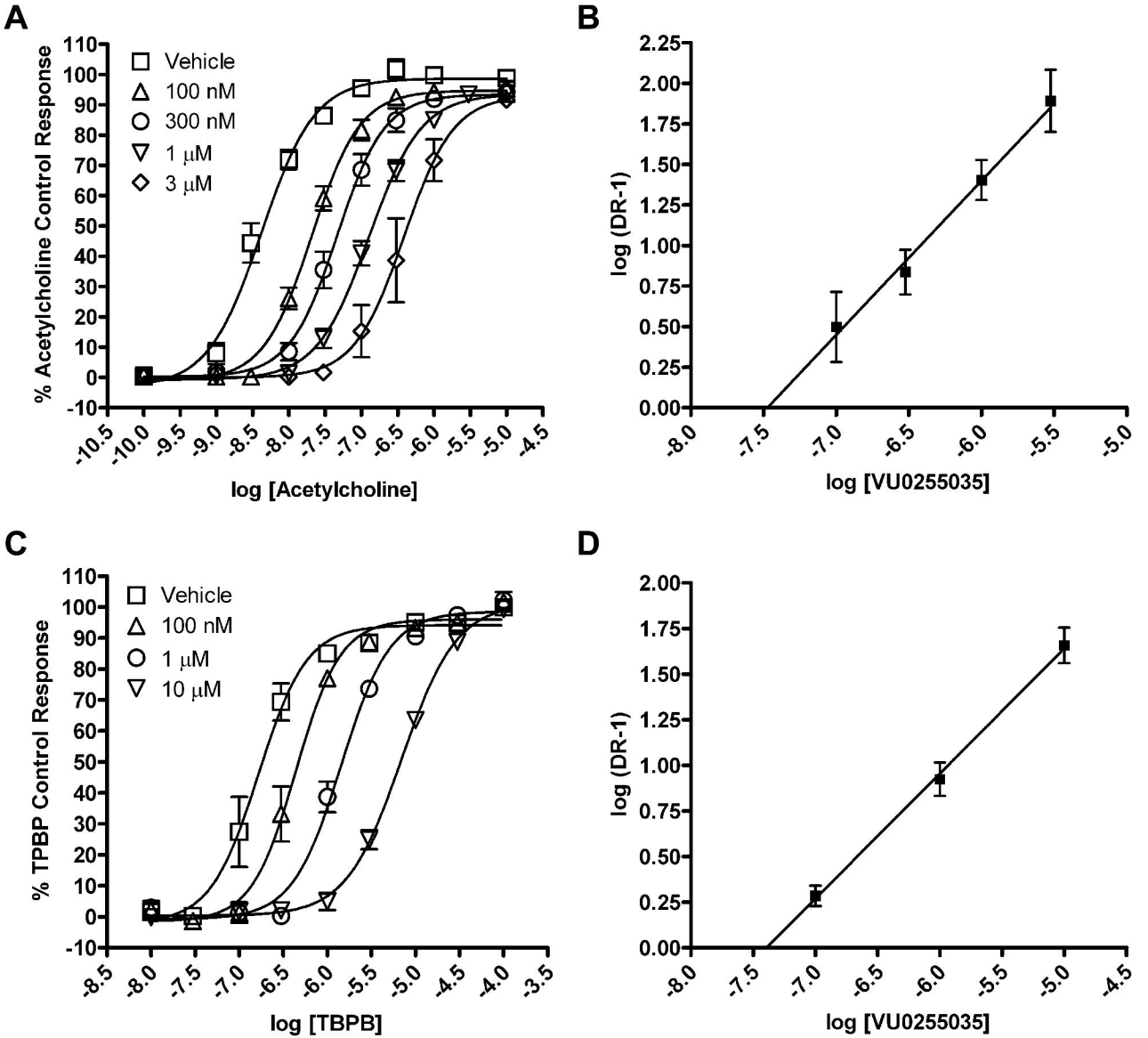
A
% Acetylcholine Control Response
Vehicle
100 nM
300 nM
1 μM
3 μM
log [Acetylcholine]
B
log (DR-1)
log [VU0255035]
C
% TPBP Control Response
Vehicle
100 nM
1 μM
10 μM
log [TBPB]
D
log (DR-1)
log [VU0255035]

Figure 7.

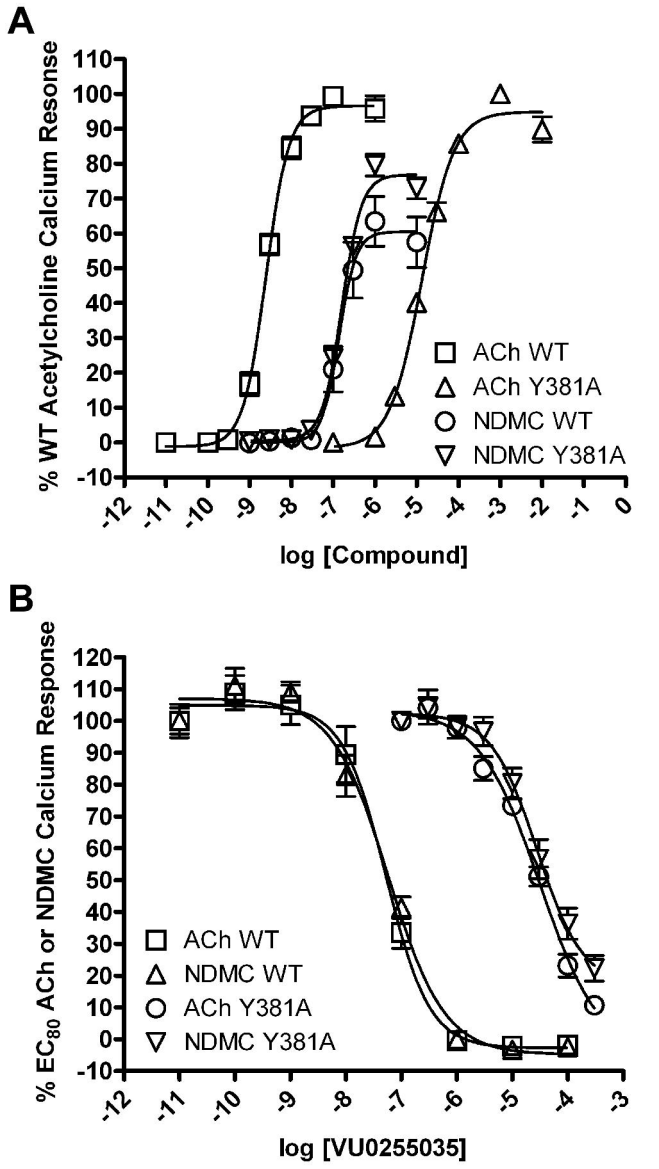
A
% WT Acetylcholine Calcium Resonse
110
100
90
80
70
60
50
40
30
20
10
0
-10
-12
-11
-10
-9
-8
-7
-6
-5
-4
-3
-2
-1
0
log [Compound]
ACh WT
ACh Y381A
NDMC WT
NDMC Y381A
B
% EC80 ACh or NDMC Calcium Response
120
110
100
90
80
70
60
50
40
30
20
10
0
-10
-12
-11
-10
-9
-8
-7
-6
-5
-4
-3
log [VU0255035]
ACh WT
NDMC WT
ACh Y381A
NDMC Y381A

Figure 8.

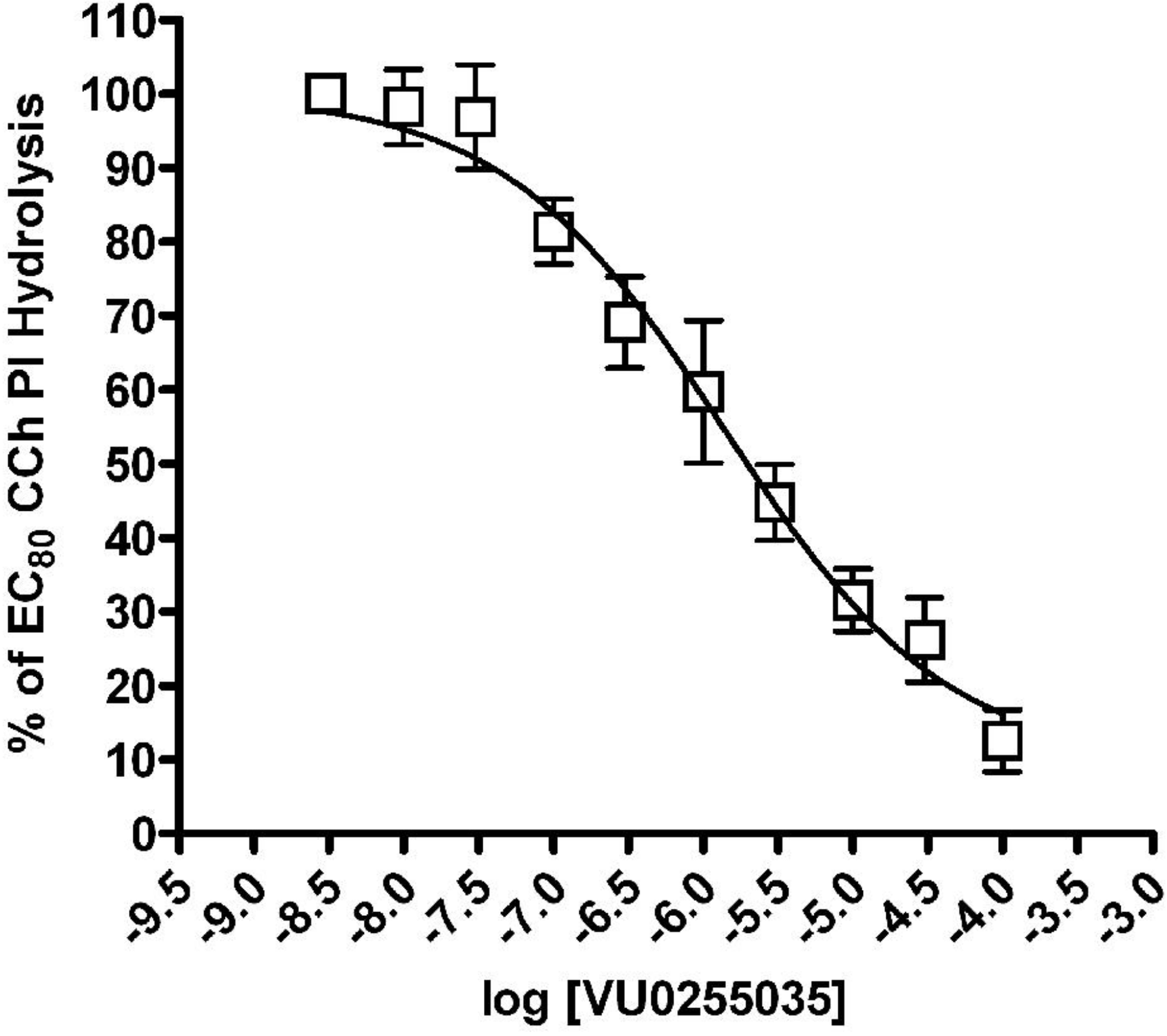
% of EC80 CCh PI Hydrolysis
110
100
90
80
70
60
50
40
30
20
10
0
-9.5
-9.0
-8.5
-8.0
-7.5
-7.0
-6.5
-6.0
-5.5
-5.0
-4.5
-4.0
-3.5
-3.0
log [VU0255035]

Figure 9.

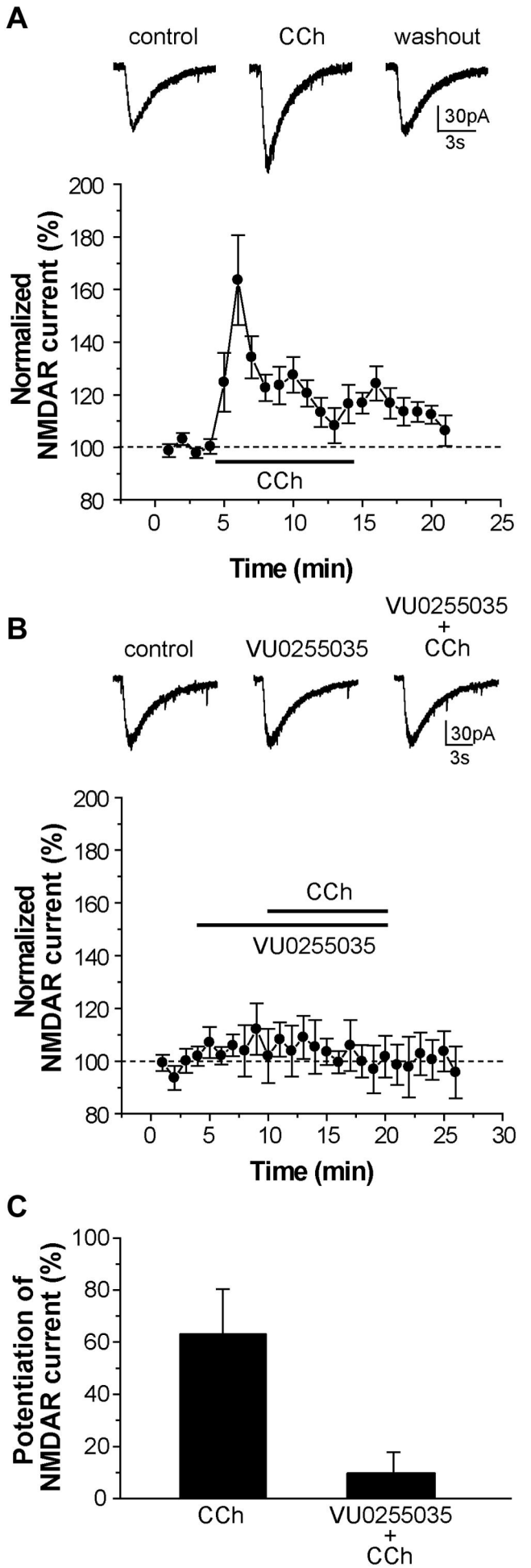
A
control
CCh
washout
30pA
3s
Normalized NMDAR current (%)
200
180
160
140
120
100
80
CCh
0
5
10
15
20
25
Time (min)
B
control
VU0255035
VU0255035 + CCh
30pA
3s
Normalized NMDAR current (%)
CCh
VU0255035
30
Time (min)
C
Potentiation of NMDAR current (%)
100
80
60
40
20
0
CCh
VU0255035 + CCh

Figure 10.

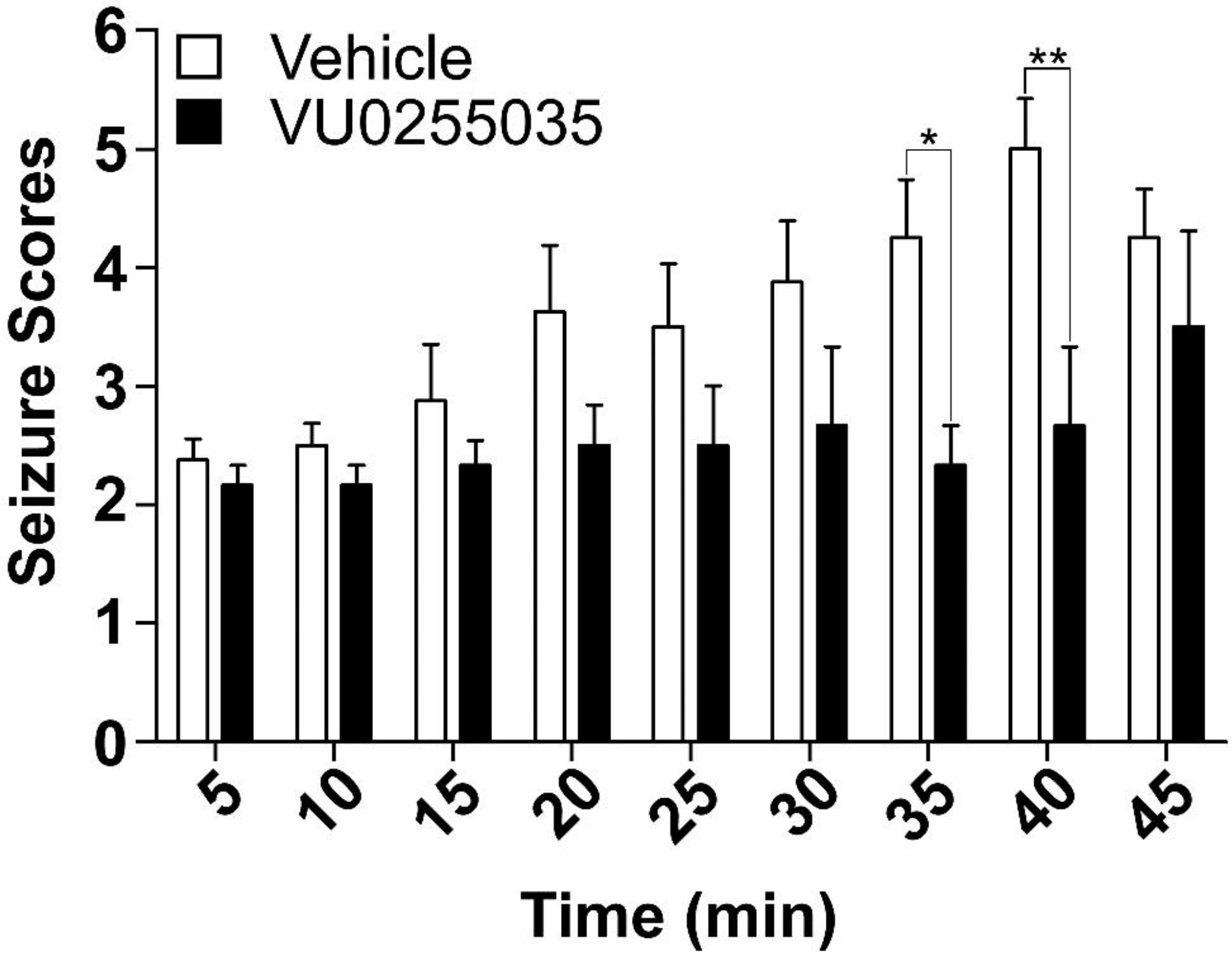
Vehicle
VU0255035
Seizure Scores
0
1
2
3
4
5
6
*
**
5
10
15
20
25
30
35
40
45
Time (min)

Figure 11.

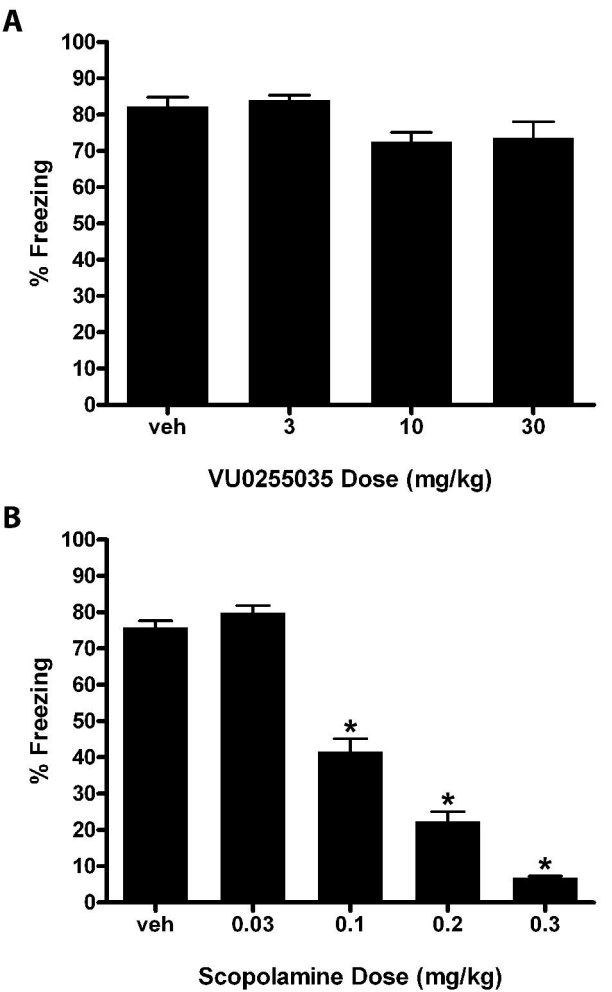
A
% Freezing
100
90
80
70
60
50
40
30
20
10
0
veh
3
10
30
VU0255035 Dose (mg/kg)
B
% Freezing
100
90
80
70
60
50
40
30
20
10
0
*
*
*
veh
0.03
0.1
0.2
0.3
Scopolamine Dose (mg/kg)